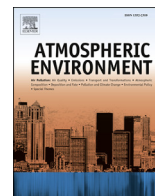




Contents lists available at ScienceDirect

Atmospheric Environment

journal homepage: www.elsevier.com/locate/atmosenv

Analysis of the WRF-Chem contributions to AQMEII phase2 with respect to aerosol radiative feedbacks on meteorology and pollutant distributions



Renate Forkel ^{a, *}, Alessandra Balzarini ^b, Rocio Baró ^c, Roberto Bianconi ^d, Gabriele Curci ^e, Pedro Jiménez-Guerrero ^c, Marcus Hirtl ^f, Luka Honzak ^g, Christof Lorenz ^a, Ulas Im ^{h, 1}, Juan L. Pérez ⁱ, Guido Pirovano ^b, Roberto San José ⁱ, Paolo Tuccella ^e, Johannes Werhahn ^a, Rahela Žabkar ^{j, g}

^a Karlsruhe Institut für Technologie (KIT), Institut für Meteorologie und Klimaforschung, Atmosphärische Umweltforschung, IMK-IFU, Kreuzeckbahnstr. 19, Garmisch-Partenkirchen, Germany

^b Ricerca sul Sistema Energetico (RSE SpA), Via Rubattino 54, Milano, Italy

^c University of Murcia, Department of Physics, Physics of the Earth, Campus de Espinardo, Ed. CIOyN, 30100 Murcia, Spain

^d Enviroware srl, Concorezzo, MB, Italy

^e Department of Physical and Chemical Sciences, Center of Excellence for the Forecast of Severe Weather (CETEMPS), University of L'Aquila, L'Aquila, Italy

^f Zentralanstalt für Meteorologie und Geodynamik, ZAMG, Hohe Warte 38, 1190 Vienna, Austria

^g Center of Excellence SPACE-SI, Ljubljana, Slovenia

^h Institute for Environment and Sustainability, Joint Research Centre, Europea Commission, Ispra, Italy

ⁱ Environmental Software and Modelling Group, Computer Science School – Technical University of Madrid, Campus de Montegancedo – Boadilla del Monte, 28660 Madrid, Spain

^j University of Ljubljana, Faculty of Mathematics and Physics, Ljubljana, Slovenia

H I G H L I G H T S

- We compare four WRF-Chem simulations which contributed to AQMEII phase2.
- Simulations include different degrees of aerosol–radiation feedback and aerosol cloud interactions.
- Lower solar radiation, temperature, PBL height, and ozone with direct aerosol effect.
- With aerosol cloud interactions higher solar radiation for clean conditions.
- Neutral on average performance except for very low aerosol concentrations.

A R T I C L E I N F O

Article history:

Received 1 June 2014

Received in revised form

28 October 2014

Accepted 30 October 2014

Available online 31 October 2014

Keywords:

WRF-Chem

Online coupled model

Direct aerosol effect

Indirect effect

Aerosol–meteorology feedback

RADM2

AQMEII-2

A B S T R A C T

As a contribution to phase2 of the Air Quality Model Evaluation International Initiative (AQMEII), eight different simulations for the year 2010 were performed with WRF-Chem for the European domain. The four simulations using RADM2 gas-phase chemistry and the MADE/SORGAM aerosol module are analyzed in this paper. The simulations included different degrees of aerosol–meteorology feedback, ranging from no aerosol effects at all to the inclusion of the aerosol direct radiative effect as well as aerosol cloud interactions and the aerosol indirect effect. In addition, a modification of the RADM2 gas phase chemistry solver was tested. The yearly simulations allow characterizing the average impact of the consideration of feedback effects on meteorology and pollutant concentrations and an analysis of the seasonality. Pronounced feedback effects were found for the summer 2010 Russian wildfire episode, where the direct aerosol effect lowered the seasonal mean solar radiation by 20 W m^{-3} and seasonal mean temperature by 0.25° . This might be considered as a lower limit as it must be taken into account that aerosol concentrations were generally underestimated by up to 50%. The high aerosol concentrations from the wildfires resulted in a 10%–30% decreased precipitation over Russia when aerosol cloud interactions were taken into account. The most pronounced and persistent feedback due to the indirect

* Corresponding author.

E-mail address: renate.forkel@kit.edu (R. Forkel).

¹ Now at Aarhus University, Department of Environmental Science, Frederiksborgvej 399, 4000 Roskilde, Denmark.

aerosol effect was found for regions with very low aerosol concentrations like the Atlantic and Northern Europe. The low aerosol concentrations in this area result in very low cloud droplet numbers between 5 and 100 droplets cm^{-1} and a 50–70% lower cloud liquid water path. This leads to an increase in the downward solar radiation by almost 50%. Over Northern Scandinavia, this results in almost one degree higher mean temperatures during summer. In winter, the decreased liquid water path resulted in increased long-wave cooling and a decrease of the mean temperature by almost the same amount. Precipitation over the Atlantic Ocean was found to be enhanced by up to 30% when aerosol cloud interactions were taken into account. The inclusion of aerosol cloud interactions can reduce the bias or improve correlations of simulated precipitation for some episodes and regions. However, the domain and time averaged performance statistics do not indicate a general improvement when aerosol feedbacks are taken into account. Except for conditions with either very low or very high aerosol concentrations, the impact of aerosol feedbacks on pollutant distributions was found to be smaller than the effect of the choice of the chemistry module or wet deposition implementation.

© 2014 The Authors. Published by Elsevier Ltd. This is an open access article under the CC BY-NC-SA license (<http://creativecommons.org/licenses/by-nc-sa/3.0/>).

1. Introduction

Aerosols are known to have an impact on weather and climate via their direct effect on radiation (Charlson et al., 1992) and via their impact on cloud formation (Twomey, 1974). These feedback processes between atmospheric aerosol particles and meteorological processes were known for quite some time and have been implemented into several regional models (e.g. Grell et al., 2011; Solomos et al., 2011; Yang et al., 2011; Bangert et al., 2011; Kushta et al., 2014). In order to account for these effects, the models are necessarily integrated or online coupled meteorology–chemistry models, i.e. both chemical and meteorological components are included in one single system. An overview of the integrated models developed and applied in the US and in Europe was given by Zhang (2008) and Baklanov et al. (2014). Dedicated applications of these models were frequently related to the investigation of feedback effects between aerosol and meteorology for dust episodes (Bangert et al., 2012; Grell et al., 2011; Kushta et al., 2014) and for regional pollution hotspots (e.g. Grell et al., 2011) during short episodes.

Until recently, simulations of regional air quality applications were mostly performed with offline models (Zhang, 2008), where the output of a meteorology simulation, which must be performed prior to the air quality simulation, is used as input for a chemistry-transport model. Consequently, these simulations cannot include feedback effects of simulated aerosol concentrations on meteorology. Therefore, aerosol–meteorology feedbacks can only be considered in integrated or online coupled meteorology–chemistry models.

A number of regional online coupled meteorology–air quality models have been developed during the last decades (e.g. Jacobson, 1997; Grell et al., 2000, 2005; Korsholm et al., 2008; Vogel et al., 2009; Mathur et al., 2010). The reasons for these developments included the desire for a more consistent description of processes such as turbulence in the meteorology and the chemistry part and for a more frequent update of the meteorological variables within the chemistry part of the model (Grell et al., 2004) as well as the desire to account for aerosol cloud interactions and aerosol radiation feedback. Generally, online-coupled meteorology–air quality models are more consistent as no interpolation in time or space is required and physical parameterizations as well as atmospheric transport are the same in the meteorology and the chemistry part (Grell and Baklanov, 2011).

With the increasing computational power, the use of online coupled meteorology–air quality models instead of separate modeling systems for meteorology and air quality became increasingly popular for regional air quality simulations. In order to

evaluate the performance of this type of model for air quality applications the second phase of the Air Quality Model Evaluation International Initiative (AQMEII <http://aqmeii.jrc.ec.europa.eu/>, Alapaty et al., 2012) concentrated on online-coupled meteorology–chemistry models, whereas the majority of models applied during the first phase of AQMEII (Solazzo et al., 2012a, 2012b; Rao et al., 2011) were offline.

For AQMEII phase2, twelve groups contributed simulations for the entire year 2010 for Europe. Among others, seven of the participating groups performed eight different simulations with WRF-Chem (Grell et al., 2005, 2011) for the European domain. Besides of its numerous physics and chemistry options, WRF-Chem also offers different choices for the degree of aerosol–meteorology interactions (http://ruc.noaa.gov/wrf/WG11/Users_guide.pdf). Prognostic aerosols enable the direct aerosol effect on radiation to be accounted for and a more explicit description of cloud–aerosol interactions, thus also accounting for the aerosol indirect radiative effect.

In order to study the impact of simulated feedback effects, the seven participating groups who applied WRF-Chem over Europe agreed upon a common setup and grid, and identical initial and boundary conditions, anthropogenic and fire emissions. The simulations differ by the chosen gas phase chemistry, aerosol module, or cloud microphysics options, and by the degree of aerosol feedback that is considered. The focus of this paper will be on four simulations using the RADM2 gas phase chemistry option (Stockwell et al., 1990) and the MADE/SORGAM aerosol module (Ackermann et al., 1998; Schell et al., 2001) of WRF-Chem. Identical physics options were chosen for these simulations. This paper adds to previous studies of feedback effect for Europe (Bangert et al., 2011; Forkel et al., 2012) in so far as it covers an entire year. This allows investigating the seasonality of simulated feedback effects and the impact of extreme pollution events such as the Russian forest fires in summer 2010.

The aim of the current paper is to investigate how aerosol meteorology interactions influence the results of WRF-Chem simulations for the European domain during an entire year and whether the inclusion of feedback effects will improve the model performance at this scale. Extensive model evaluation studies for the meteorological variables, ozone, and particulate are presented by Brunner et al. (2015), Im et al. (2015a, 2015b). Therefore, the scope of this paper is mostly restricted to the discussion of the impact of aerosol meteorology feedback effects and discussion of the impact of the modification of the RADM2 solver.

Further simulations using WRF-Chem's CBMZ–Mosaic option, a VBS secondary aerosol module, and a different cloud microphysics module are discussed in companion papers (San José et al., 2015; Makar et al., 2015a, 2015b; Baró et al., 2015).

2. Setup of the simulations

The simulations for Europe discussed here were performed using WRF-Chem version 3.4.1 with identical physics options, grid spacing, and input.

The choice of the physics and chemistry options can have a strong impact on the quality of the results. Given the lengths of the simulation period and the deadlines for the AQMEII model inter-comparison in particular, the choice of chemistry options was strongly constrained by the computational costs. However, the chosen options are widely used in the community.

The following physics options were applied for the simulations: Rapid Radiative Transfer Method for Global (RRTMG) long-wave and short-wave radiation scheme (Iacono et al., 2008), Yonsei University (YSU) PBL scheme (Hong et al., 2006), NOAA land-surface model (Chen and Dudhia, 2001) and the Grell 3D ensemble cumulus parameterization (Grell and Devenyi, 2002) with radiative feedback.

For all simulations, the same grid spacing of 23 km was applied with 270 by 225 grid cells (Lambert Conformal Conic projection with center at 50N and 12E). The modeling domain covers Europe, the North Atlantic and a portion of Northern Africa, as well as large areas affected by the Russian forest fires. In the vertical direction, the atmosphere up to 50 hPa is resolved into 33 layers with a higher resolution close to the surface.

According to the common simulation strategy for AQMEII phase2, the entire year 2010 was simulated as a sequence of two-day time slices. In this way, the development of semi-direct effects, i.e. changes in the cloud distribution due to changes in the radiation budget, could be constrained without making use of nudging for the meteorological variables. The chemical initial state at the beginning of each time slice is adopted from the final state of the previous time slice, while meteorology is reinitialized every two days. The last five days of the year 2009 were used as spin-up for the chemistry.

Initial- and boundary-conditions for the meteorological variables were obtained from 3-hourly data with 0.25° resolution (analysis at 00 and 12 UTC and respective forecasts at 03/06/09/15/18/21 UTC) from the ECMWF operational archive. Three-hourly chemistry boundary conditions for the main trace gases and particulate matter concentrations were available from the ECMWF IFS-MOZART model run from the MACC-II project (Monitoring Atmospheric Composition and Climate, Inness et al., 2013) with a grid width of 1.125°.

Anthropogenic emissions for the EU domain were provided by the TNO (Netherlands Organization for Applied Scientific Research) from a recent update of the TNO MACC emissions inventory (<http://www.gmes-atmosphere.eu/>; Kuenen et al., 2014; Pouliot et al., 2012, 2015).

Biomass burning emission data were calculated from global fire emission data with spatial resolution of 0.1° × 0.1° supplied from the project “Integrated monitoring and modelling system for wild-land fires” (IS4FIRES, Sofiev et al., 2009). Day and night vertical injection profiles were also provided. WRF-Chem emission species were calculated by speciation following Andreae and Merlet (2001) and Wiedinmyer et al. (2011). Following common practice for simulations with large grid widths, no heat release due to the fires was taken into account. According to the directives for the AQMEII phase2 simulations no volcanic emissions were considered in spite of the Eyjafjallajökull eruption in spring 2010.

Biogenic emissions are based on MEGAN (Model of Emissions of Gases and Aerosols from Nature, Guenther et al., 2006). MEGAN is online coupled with WRF-Chem and makes use of simulated temperature and solar radiation. Dust emissions were modeled

according to Shaw et al. (2008), with an adjustment to avoid extremely high desert dust fluxes.

The chemistry options and the differences in the setup of the WRF-Chem simulations for AQMEII phase2 for the European domain are summarized in Table 1. The focus of the paper is on the four simulations using the RADM2 gas phase chemistry (Stockwell et al., 1990) and the MADE/SORGAM aerosol module (Ackermann et al., 1998; Schell et al., 2001) with different degrees of aerosol meteorology interactions. The remaining four WRF-Chem simulations with a different cloud module or different chemistry and aerosol options are also included in the table as their results will also be consulted for comparison. Photolysis frequencies are from Fast-J (Wild et al., 2000) for all simulations. With the exception of the ES1 simulation using the cloud microphysics of Lin et al. (1983), identical physics options were chosen.

The simulation SI2, which does not include any explicit aerosol–meteorology interactions at all, is considered the baseline case. Case SI1 includes only the aerosol direct effect on radiation according to Fast et al. (2006) and Chapman et al. (2009). For the cases SI2 and SI1, cloud droplet formation does not depend on the simulated aerosol particle numbers and WRF's standard configuration with a fixed value of 250 cloud droplets per cm³ is applied in the cloud microphysics module. The cases AT1 and DE4 additionally include aerosol cloud interactions for grid scale clouds using a two-moment cloud microphysics scheme (Yang et al., 2011). Therefore also the aerosol indirect radiative effect is included. Aerosol activation in grid scale clouds is based on the parameterization of Abdul-Razzak and Ghan (2002). The inclusion of the aerosol cloud interactions for grid scale clouds (Chapman et al., 2009; Yang et al., 2011) also affects grid scale precipitation and allows for a more explicit description of the wet deposition.

DE4 and AT1 differ by the complexity of the applied liquid phase chemistry of grid scale clouds, using the Walcek and Taylor (1986) and Fahey and Pandis (2001) liquid phase chemistry module, respectively. The Walcek and Taylor model includes the description of aqueous phase sulfate production in the bulk phase. The computationally inexpensive bulk approach underestimates aqueous sulfate formation for many conditions since it cannot account for the dependence of the droplet's pH value on droplet size. In order to improve upon this weakness of the bulk approach, the Fahey and Pandis (2001) model combines the bulk approach with a two-section size-resolved approach. In the convective parameterization, the Walcek and Taylor (1986) bulk aqueous phase chemistry is included for all simulations discussed here.

DE4 also includes a modification of the RADM2 gas phase chemistry solver. The other three simulations with RADM2 gas phase chemistry were all performed with the QSSA chemistry solver for RADM2 as it is supplied with WRF-Chem. Compared to observations and simulations with other chemistry mechanisms and solvers, the WRF-Chem version of the RADM2 QSSA solver underestimates ozone titration in areas with high NO emissions (Supplement, Fig. S1). Therefore, an attempt was made to improve the description of the ozone titration within this solver. Details of this modification are given in the Appendix. As will be shown later in this paper, the AQMEII phase2 study revealed that the modification results in an over-estimation of the ozone concentrations.

The current analysis is based on the model outputs that have been submitted to the ENSEMBLE system (Bianconi et al., 2004; Galmarini et al., 2012) by the different groups participating in AQMEII phase2.

3. Results and discussion

Essentially, the performance of the WRF-Chem simulations for Europe was comparable to most of the other participating models

Table 1

Configuration of all AQMEII phase2 simulations for Europe with WRF-Chem. The first four columns summarize the setup of the simulations discussed in this paper.

	SI2 (Baseline)	SI1	DE4	AT1	ES1	IT2	IT1	ES3
Version	3.4.1	3.4.1	3.4.1	3.4.1	3.4.1	3.4 with 3.5 VBS	3.4.1	3.4.1
Microphysics	Morrison ^a	Morrison ^a	Morrison	Morrison	Lin ^b	Morrison	Morrison	Morrison
Gas phase chem.	RADM2 ^c	RADM2	RADM2 modified	RADM2	RADM2	RACM ^d	CBMZ ^e	CBMZ
Inorg. aerosol	MADE ^f	MADE ^f	MADE	MADE	MADE	MADE	MOSAIC ^g	MOSAIC
Org. aerosol	SORGAM ^h	SORGAM ^h	SORGAM	SORGAM	SORGAM	VBS ⁱ	–	–
Grid scale wet deposition	Simple	Simple	Easter, 2004 ^j	Easter, 2004	Easter, 2004	Easter, 2004	Simple	Easter, 2004
Grid scale aq. chemistry	–	–	WT ^k	FP ^l	FP	WT	–	FP
Aerosol direct radiative effect	No	Yes	Yes	Yes	Yes	Yes	No	Yes
Aerosol–cloud interactions and indirect effect	No	No	Yes	Yes	Yes	Yes	No	Yes

^a Morrison et al., 2009.^b Lin et al., 1983.^c Stockwell et al., 1990.^d Stockwell et al., 1997.^e Zaveri & Peters 1999.^f Ackermann et al., 1998.^g Zaveri et al., 2008.^h Schell et al., 2001.ⁱ Ahmadov et al., 2012.^j Easter et al., 2004.^k Walcek & Taylor 1986.^l Fahey & Pandis 2001.

(Brunner et al., 2015; Im et al., 2015a, 2015b) in spite of the preference for the more simple physics and chemistry options in WRF-Chem. Except for the wind speed, meteorological results were similar to or better than those of the other participating models.

Although wind speed was over-predicted by the majority of the models (Brunner et al., 2015), the over-prediction by 25–35% for the WRF-Chem simulations is on the high side. WRF is generally known to over-predict in particular at low to moderate wind speeds, not only for the simple but also for the more complex boundary layer schemes. This over-prediction can be partly attributed to unresolved topography such as hills and valleys and other smaller scale terrain features by the default surface drag parameterization (Jimenez and Dudhia, 2012, Mass and Ovens, 2011). It may also be speculated that the choice of surface parameters, the choice of the land surface model, the vertical model resolution, and the way how the 10 m wind speed is interpolated from the values at grid points may have an effect.

Annual domain-mean ozone concentrations were reproduced by the simulations using the RADM2 mechanism with a normalized mean bias between –5% for AT1 and –1.6% for DE4 and correlations around 0.85 for all simulations. For DE4, almost 10 ppbv higher ozone concentrations were found in the Southern part of the modeling domain compared to those of the simulations with the unmodified RADM2 solver.

Fig. 1 shows the simulated seasonal mean distribution of PM₁₀ during 2010 for the baseline case SI2. PM₁₀ concentrations were generally underestimated in all simulations with a normalized mean bias of –22%/–49% for SI2 and SI1 and –43%/–61% for AT1 and DE4 for rural/urban stations, respectively (Im et al., 2015a,b). For PM_{2.5}, the performance was better with normalized mean biases of –9%/–27% and –31%/–45%, respectively. Similar under-predictions were not only found for WRF-Chem but also for the majority of models participating in AQMEII phase2. Besides a possible underestimation of anthropogenic emissions, this under-prediction may partly be attributed to the comparatively coarse resolution, which does not resolve urban pollution hotspots. Furthermore, the overestimation of the wind speed can result in a too fast removal of pollutants from urban areas.

Due to the importance of the Russian wild fire emissions, a strong focus of the following discussion is on the summer season. This is also reflected in the choice of figures. Figures for seasons

other than summer are only included in the paper if the feedback effects vary strongly with season. However, complete sets of figures for all seasons are provided in the [Supplementary material](#).

3.1. Impact of aerosol feedback on meteorological variables

3.1.1. Radiation

The simulated summer 2010 average of the global radiation for the baseline case without any aerosol meteorology feedbacks (case SI2) is shown in the upper part of Fig. 2. Due to the typical persistent cloud layer over the North Atlantic the lowest solar radiation is found in this region.

The middle and lower parts of Fig. 2 show the mean differences for summer 2010 between the cases with aerosol meteorology feedback and the baseline case. Consideration of the direct aerosol effect (case SI1) results in a reduction of the solar radiation throughout the model domain for all seasons. During the summer, the average global radiation is 10–20 W m^{–3} or 5% lower in the Southern part of the modeling domain when the direct aerosol effect is considered. This can be attributed to high dust concentrations in this area. Over the North Atlantic the incoming solar radiation is only 2% lower for case SI1 than for the baseline case. Over Russia, the high aerosol concentrations due to the forest fires between July 25th and August 19th reduced the summer average of the global radiation by up to 25 W m^{–3}. On single days, the solar radiation in the fire region was attenuated by 100 W m^{–2} (see also Kong et al., 2015).

Urban aerosol emissions contributed to an additional local reduction by only 1–2 W m^{–2} or 2–3% in the summer. Therefore, the effect of urban anthropogenic PM emissions for major cities or the Po valley in northern Italy cannot be recognized in Fig. 2. Due to the underestimation of anthropogenic aerosol concentrations for urban areas in the model simulations (Im et al., 2015a,b), this effect is only comparatively weak and probably also underestimated.

The current results for the impact of the direct aerosol effect seem to differ from the results of Forkel et al. (2012), who performed a continuous simulation over two months. This continuous simulation allowed the development of semi-direct effects, i.e. the absorption of solar radiation could induce subsequent changes in PBL height, cloud cover, and precipitation. In the current study, the restart of the meteorology every two days constrains the development of semi-direct effects and the propagation of feedback

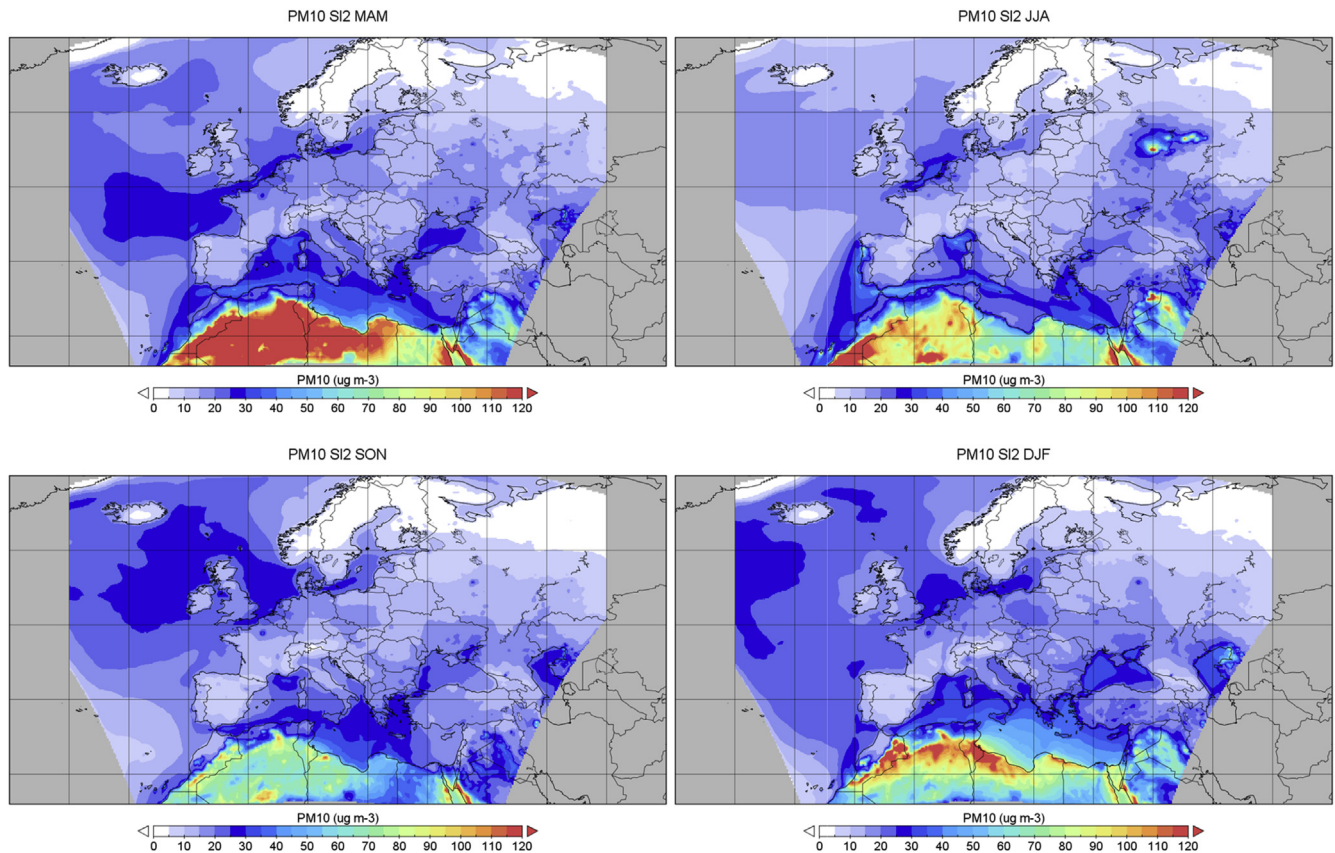


Fig. 1. Seasonal mean PM_{10} in $\mu\text{g m}^{-3}$ for the baseline case SI2 for spring (MAM), summer (JJA), fall (SON), and winter (DJF).

effects. An exception is the region of the Russian forest fires in July and August, where the strong attenuation of solar radiation due to high and temporally variable aerosol concentrations induced a faster development of semi-direct effects. However, the occurrence of semi-direct effects during this episode is only visible as irregular pattern in the daily fields of solar radiation and is not visible in the seasonal mean of the solar radiation.

When comparing results where the aerosol indirect effect is considered with the baseline case, the most striking feature is the strong increase in solar radiation over the Atlantic and Northern Europe. Since similar results were found for AT1 and DE4, only DE4 is displayed in Fig. 2. Simulated aerosol particle numbers over the Atlantic are only in the range of only 1000–3000 particles per kg of air. When aerosol cloud interactions are considered, this results in simulated cloud droplet numbers between 5 and 100 cm^{-3} . If simulated aerosol concentrations are not taken into account for cloud droplet formation, a standard value of 250 cloud droplets per cm^{-3} is assumed for the entire modeling domain in the standard configuration of WRF. This assumption, which is more typical for continental conditions, results in a liquid water path and a cloud optical depth over the North Atlantic for the cases SI1 and SI2, which is almost twice as high as for the cases AT1 and DE4. The lower liquid water paths for cases AT1 and DE4 lead to a 40% increase in the summer average global radiation over the North Atlantic. In spring, a relative increase of 25% was found, in autumn ca. 20%, and in winter the solar radiation was only 10% higher for AT1 and DE4 than for the baseline case.

A small reduction in the cloud liquid water path in summer was found for the cases AT1 and DE4 even for central Europe. As a result, the decrease in solar radiation due to the direct aerosol effect can be partly compensated when the indirect effect is included. An

exception is the region of the Russian forest fires, where very high aerosol concentrations occurred and cloud droplet numbers were higher than for cases SI1 and SI2 during the fire episode.

The differences between the simulated liquid water paths and global radiation for the cases AT1 and DE4 and the baseline case are similar to the patterns found for other cases including aerosol cloud interactions (cases ES1, IT2, and ES3). This indicates that the reduction of the cloud liquid water path and the resulting increase of the global radiation are independent of the applied aerosol module and cloud microphysics module (Baró et al., 2015; San José et al., 2015). Previous tests indicated that this effect will still persist for aerosol concentrations over the North Atlantic that are twice as high as those simulated here. As shown by Forkel et al. (2012), the reduction in cloud optical depth can result in better agreement between observed and simulated solar radiation for cloudy conditions in regions with low aerosol concentrations like Northern Europe.

Considering the seasonal variability of the incoming solar radiation and the presence or absence of extreme PM concentrations (e.g. from the Russian wildfire emissions) the effect was similar for the other seasons (figures for all seasons are shown in the Supplement).

However, it has to be emphasized, that the differences in cloud optical depths and global radiation between simulations with and without aerosol cloud interactions will depend to some extent on the assumed baseline droplet concentrations if no explicit aerosol cloud interactions are included. In the standard configuration of WRF and WRF-Chem 3.4.1, continental conditions were implicitly assumed for the entire modeling domain if cloud droplet formation is not explicitly calculated from predicted aerosol particle numbers. More realistic aerosol fields for the baseline case instead of

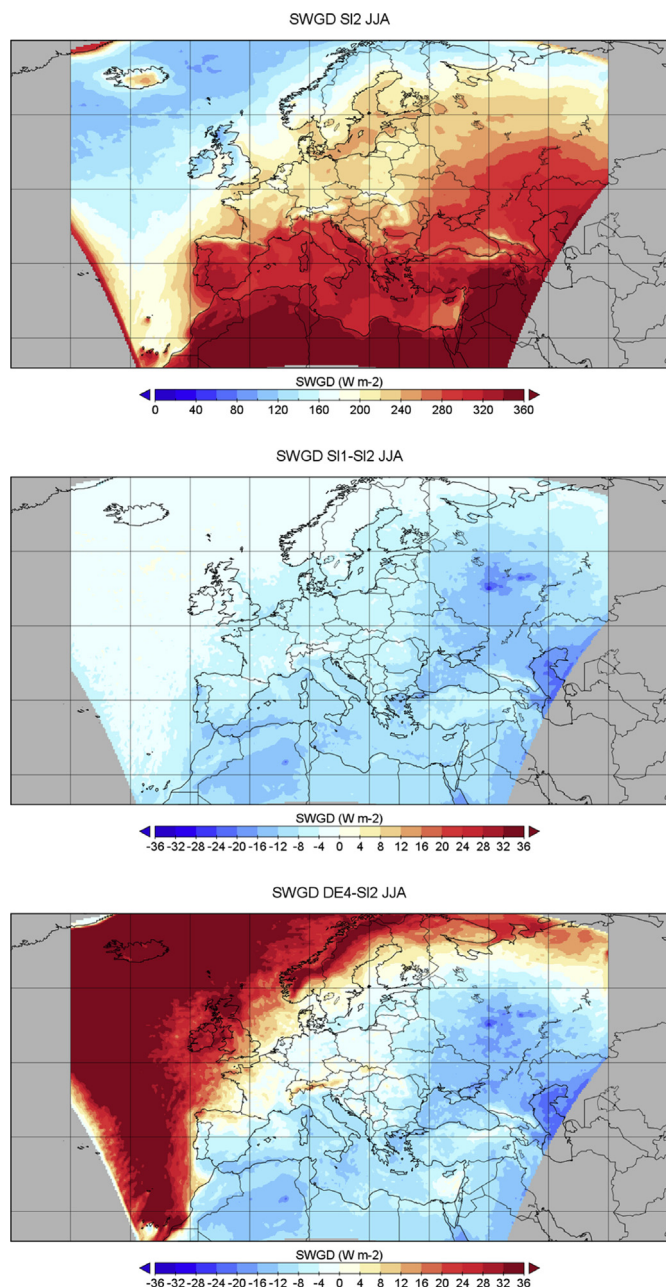


Fig. 2. Seasonal mean solar radiation for summer 2010 in W m^{-2} . Top: Baseline; center: difference between case SI1 with direct aerosol effect and baseline; bottom: difference between case DE4 with direct plus indirect aerosol effect and baseline.

horizontally homogeneous particle numbers would therefore improve the model's performance for unpolluted conditions and reduce the differences between simulations where aerosol cloud interactions depend on simulated aerosol concentrations and the baseline. This option, which is available since the WRF version 3.6, was not yet available for the current study. On the other hand, effects may probably be even more pronounced if aerosol cloud interactions were also included in the sub-grid convective cloud parameterizations.

3.1.2. Temperature and PBL height

The simulated seasonal mean temperature was found to decrease due to the direct aerosol effect by $0.1\text{--}0.3^\circ$ (Fig. 3), with

the patterns mostly reflecting the patterns of decreased solar radiation. The temperature decrease was more pronounced in summer than in winter. Although the dust concentration over Northern Africa was highest in the spring, the effect on temperature was slightly stronger in the summer due to the higher solar radiation (Supplement, Fig. S3). The aerosol emitted by the Russian forest fires resulted in a decrease of the mean summer temperature by 0.4° . Looking at single days, a maximum reduction by almost one degree was found (not shown). Note that no heat release due to the fires was considered in the simulations.

The additional inclusion of aerosol cloud interactions and the indirect aerosol effect result in an additional temperature decrease for the major part of the modeling domain. In spite of the higher solar radiation over the North Atlantic, lower near surface temperatures were found there. This can be attributed to the combined effect of the prescribed sea surface temperature and enhanced precipitation. The temperature decrease was most pronounced during the summer.

Over Northern Europe, the simulated strong increase in solar radiation for the cases including aerosol cloud interactions and the indirect aerosol effect results in higher mean summer temperatures by up to 1° . However, a decrease of the cloud liquid water path not only results in increased solar radiation but can also lead to enhanced cooling due to long-wave radiation. Since solar radiation is very low in Northern Europe during winter, the cooling due to the increased outgoing long-wave radiation becomes dominant. Therefore, winter temperatures in Scandinavia were up to one degree lower for cases DE4 and AT1 than for those cases where no aerosol cloud interactions were taken into account (Fig. 3, lower right). For spring and autumn, temperatures that were between 0.2 and 0.4° lower were found over Scandinavia (See electronic supplement, Fig. S3).

The large scale patterns of the summertime temperature differences shown in Fig. 3 are strongly reflected in the patterns of changes in PBL height (Fig. 4). The small mean additional direct aerosol effect for anthropogenic pollution hotspots of only -1 to -2 W m^{-2} led to mean PBL heights that were $5\text{--}8 \text{ m}$ lower than in the surrounding regions during the spring and summer. However, except for the Po valley in Northern Italy, this effect is not visible in the seasonal mean differences due to the small extension of these local minima. When the indirect aerosol effect is also considered, this small effect of urban areas is additionally masked by changes in the cloud optical depth. Furthermore, lower PBL heights are found over the Channel and the Mediterranean in spite of the slightly increased or unchanged near surface temperatures.

3.1.3. Precipitation

Aerosol cloud interactions and the subsequent impact on precipitation can be considered to be on the highest rank of the most important meteorology and chemistry interactions (Baklanov et al., 2014). For the current case studies, the inclusion of aerosol cloud interactions had a strong effect on simulated cloud droplet number concentrations and resulted in a pronounced increase of the precipitation over the North Atlantic for all seasons. Since the evaluation data set used by Brunner et al. (2015) is restricted to land surfaces, an additional comparison of the simulated precipitation against the GPCP (Global Precipitation Climatology Project, <http://www.esrl.noaa.gov/psd/data/gridded/data.gpcp.html>) data set was performed. The GPCP data set with a horizontal resolution of 2.5° also covers the ocean, which is not the case for the better 25 km resolution E-OBS data set (<http://www.ecad.eu>, Haylock et al., 2008). GPCP is a merged data set from satellite and gauge data supplied by NOAA ESRL. For the comparison, the model results were interpolated on the grids of the observational data.

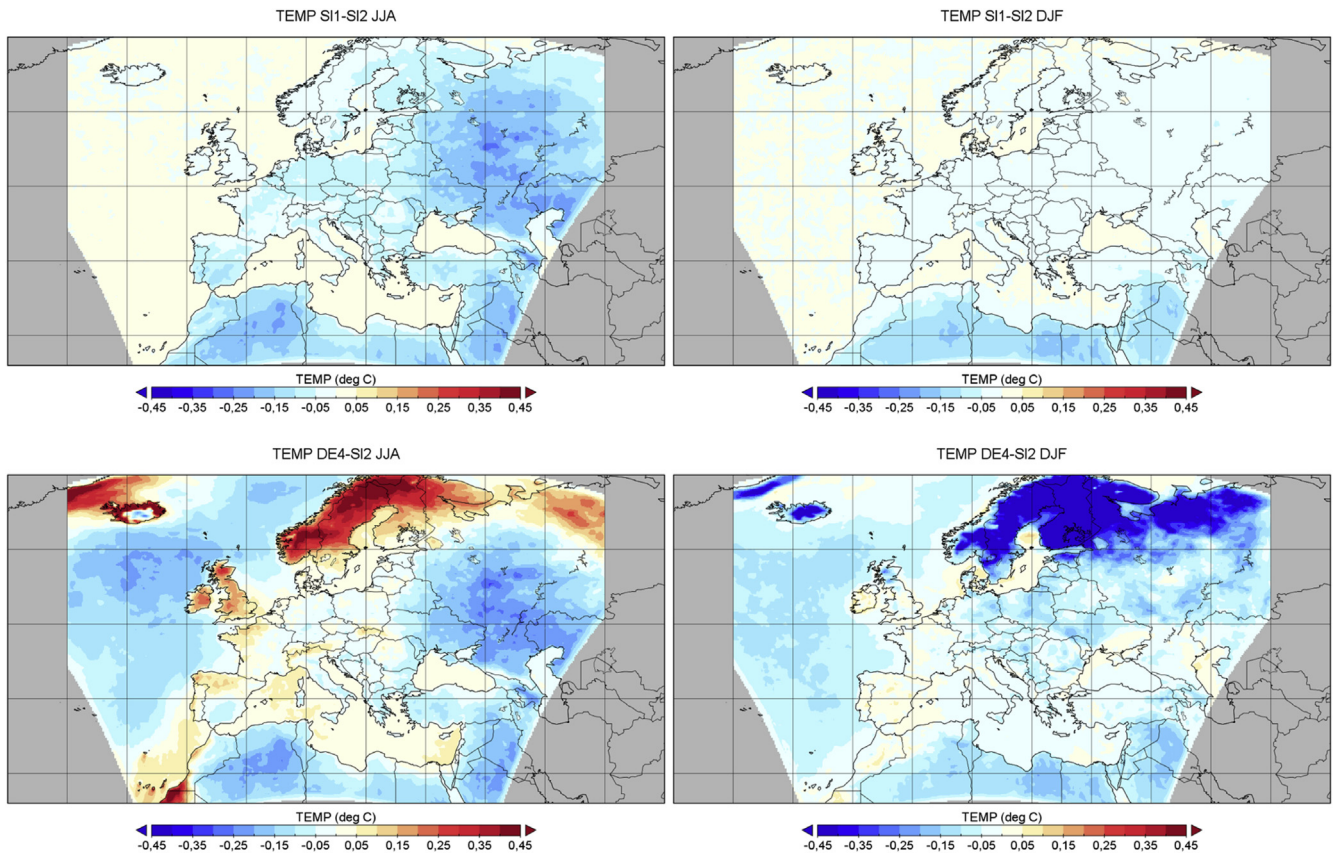


Fig. 3. Seasonal mean temperature difference between case S11 and S12 (top) and between DE4 and S12 (left) for summer (top) and winter (right).

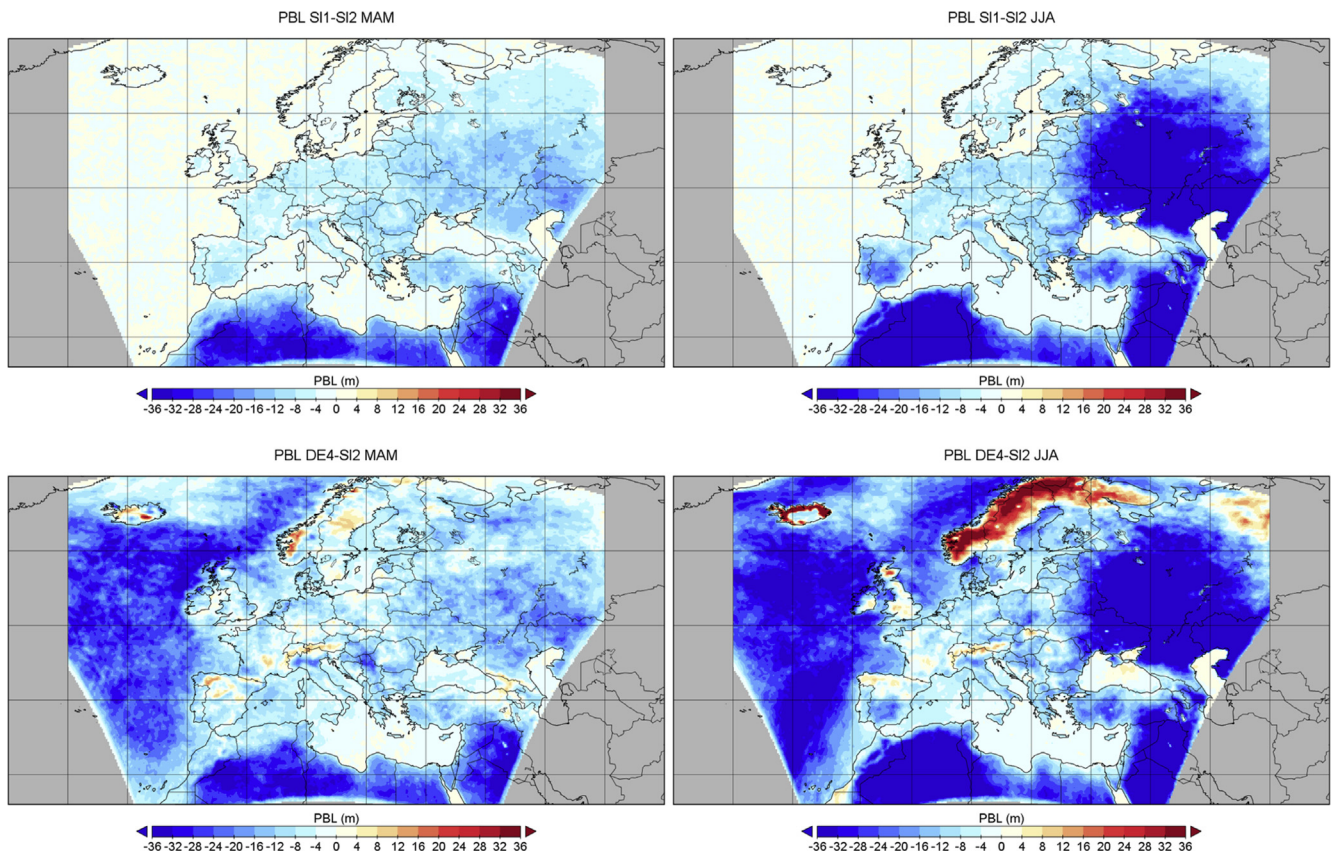


Fig. 4. Seasonal mean PBL height difference between case S11 and baseline (top) and between DE4 and baseline (bottom) for spring (left) and summer (right).

The overall spatial patterns of the summertime precipitation for the baseline case compare well to the GPCP observations, although the amount of seasonal accumulated precipitation was lower than observed in the Western part of the modeling domain and higher in the Eastern part (Fig. 5). It still remains to be investigated whether this can be attributed to a higher relevance of the ice phase during these seasons. For the other seasons, precipitation was higher than observed over the Atlantic (Fig. S6). For the entire domain, the domain average bias of precipitation for case SI2 is -6% in spring and between -2% and $+2\%$ for the other seasons. The spatial correlation was around 0.8 in spring and fall, almost 0.9 in summer, and 0.77 in winter. Similar results as for the comparison with the GPCP data were found over land surfaces for the E-OBS data set (not shown). Also, the monthly variability in precipitation is well captured (Brunner et al., 2015).

Compared to the base case SI2, the inclusion of the direct aerosol effect (case SI1) only results in small changes of seasonal precipitation. An exception is the Eastern part of the model domain during the summer, where the monthly precipitation is decreased locally by 10 mm. Elsewhere and during the other seasons, the deviations were between -3 mm and $+3$ mm without showing any pronounced pattern. Changes in bias and correlation for the entire model domain were only marginal.

The additional inclusion of aerosol cloud interactions and the indirect aerosol effect for grid scale clouds resulted in a further reduction of precipitation in the summer over Russia by further 5 mm (Fig. 5 shows the difference between case DE4 and SI2; very similar patterns were found for the case AT1), which corresponds to a decrease by 20% as compared to the baseline. The increase in precipitation over the North Atlantic and Northern Europe, i.e. for regions with very low aerosol and CCN concentrations, is more pronounced. For case DE4, CCN column number concentrations of only $2 \cdot 10^7$ to $1 \cdot 10^8$ cm^{-2} were found over the North Atlantic as compared to $5 \cdot 10^8$ to $1 \cdot 10^9$ cm^{-2} over the European continent. For AT1 and DE4, precipitation over the North Atlantic is 10–30% higher than for SI2. Increased precipitation for pristine conditions was also reported by Solomos et al. (2011). For summer in particular, inspection of the large scale patterns shows a slightly better agreement with observations over land when aerosol effects were included.

Over the North Atlantic, accounting for aerosol cloud interactions results in a slight improvement of the bias (change from -10% to 1%) and the correlation (change from 0.7 to 0.75) between the simulations and the GPCP analysis during the summer. For the other seasons, the inclusion of aerosol cloud interactions resulted in a change of the bias for the worse by the same amount and an almost unchanged correlation.

The deviations from the baseline due to the inclusion of aerosol effects are generally smaller than differences due to the application of a different cloud microphysics scheme (case ES1). These differences are discussed in a companion paper (Baró et al., 2015).

It must also be taken into account that aerosol cloud interactions are only considered for the grid scale precipitation. For convective precipitation, these interactions were not yet included in the WRF-Chem version 3.4.1. Over water surfaces, and in particular during the summer also over land, the convective precipitation contributes approximately 50% to the total precipitation.

3.2. Impact of aerosol feedback on pollutant concentration

3.2.1. NO_2 and ozone

The direct aerosol effect results in a small positive deviation of the NO_2 concentration for most of the model domain (Fig. 6).

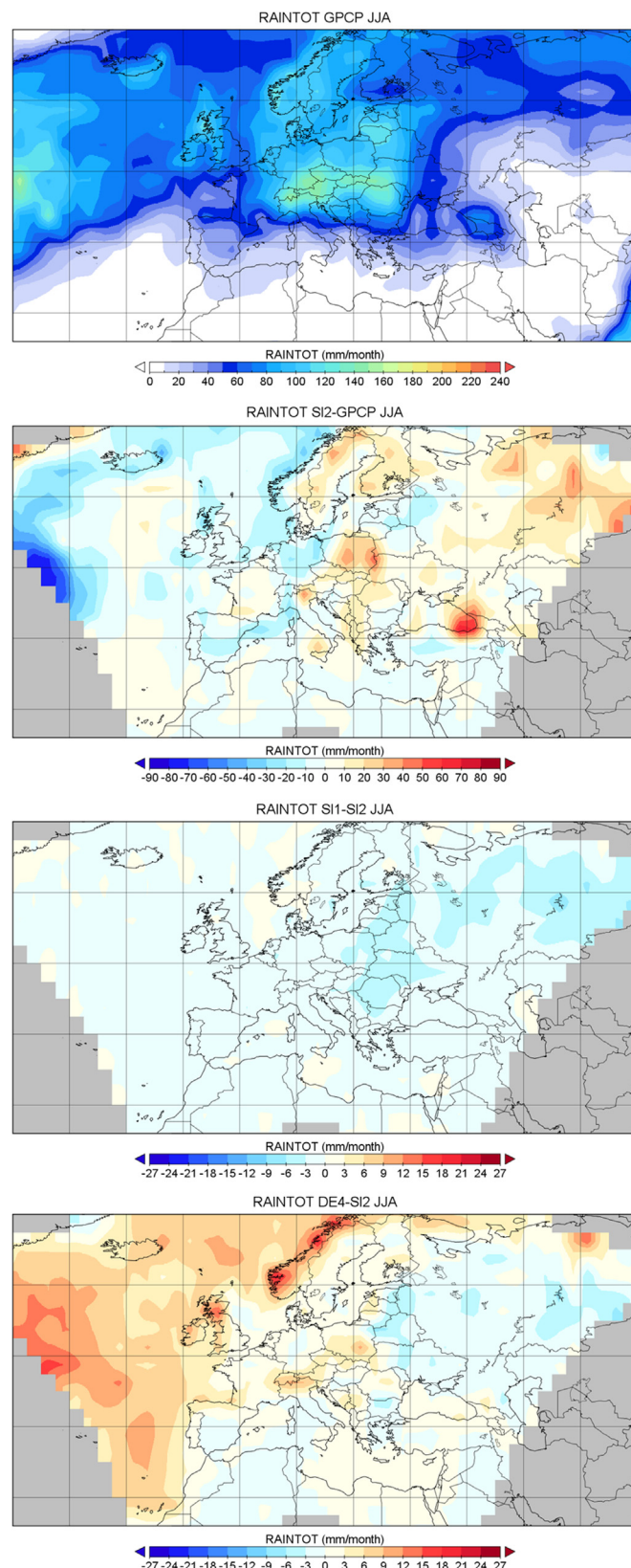


Fig. 5. Mean monthly precipitation in mm for summer 2010. Model results are interpolated to the $2.5^\circ \times 2.5^\circ$ grid of the GPCP observational data. Top to bottom: GPCP observational data; difference between SI2 (baseline, no aerosol feedback) and GPCP; difference between SI1 (direct aerosol effect) and baseline; difference between DE4 (direct aerosol effect plus aerosol–cloud interactions) and baseline.

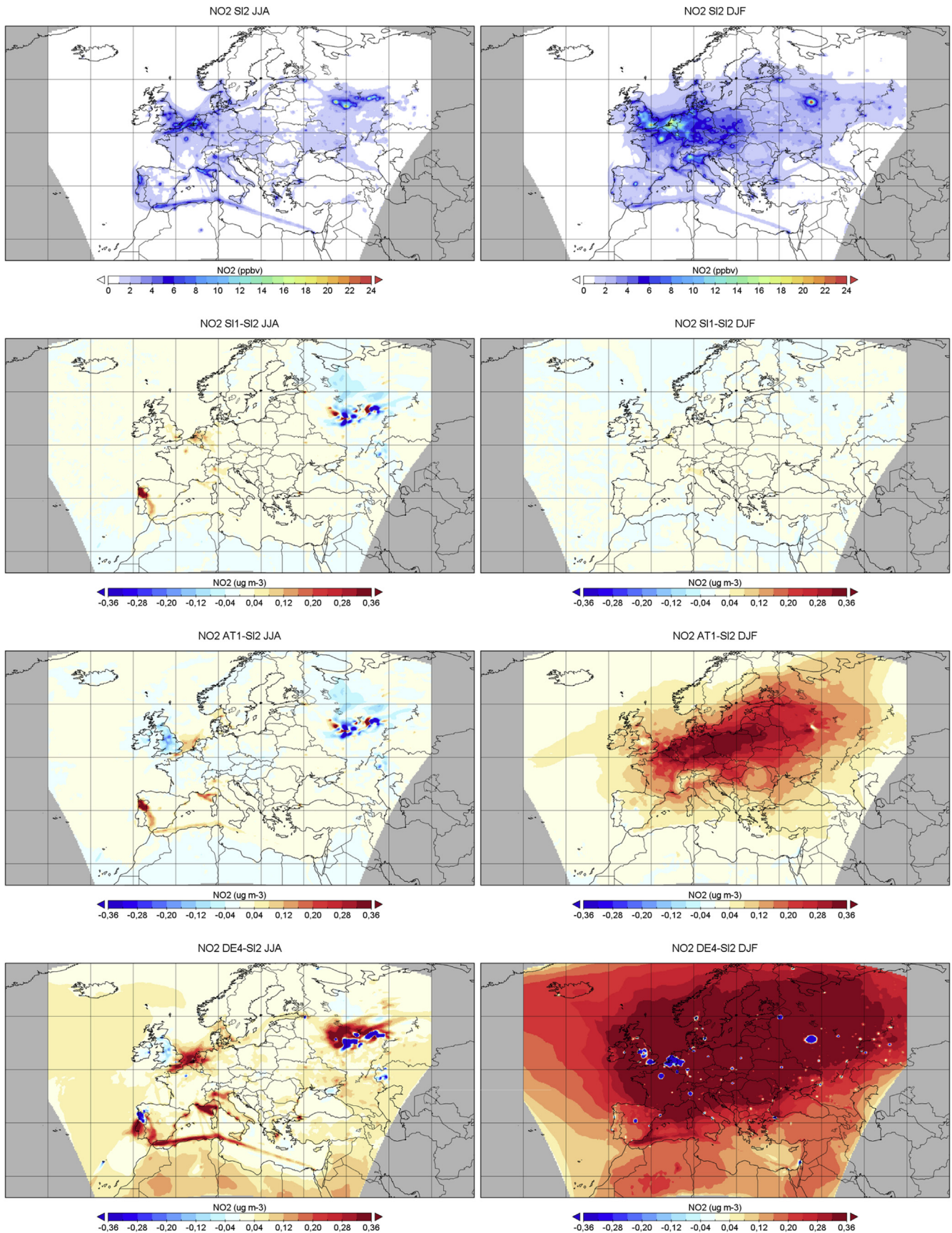


Fig. 6. Seasonal mean NO₂ concentration in ppbv for summer (left) and winter (right). From top to bottom: Baseline concentrations; difference between SI and baseline; difference between AT1 and baseline; difference between DE4 (same as AT1 but with different aqueous phase chemistry and modified gas phase solver) and baseline. The maximum value for DE4-SI2 is 1.04 ppbv, the minimum value is -22 ppbv.

Although the simulated reduction of the mean PBL height for pollution hotspots like Paris, Moscow, the Po valley, or the forest fire region in Portugal is only small, NO₂ concentrations are increased by 1–5 % for these areas. In spite of a 50–80 m lower average PBL height over the region of the Russian forest fires for case SI1, NO₂ concentrations did not increase throughout this area. The changing patterns of the fire and short term changes of the PBL height can result in regional increases and decreases of the summertime average NO₂ by ± 0.5 ppb. Peak deviations of 50 ppb between case SI1 and the baseline simulation were found during the fire episode due to temporal and local shifts of the fire plume.

For case AT1, the small increase in NO₂ concentration which was found for SI1 is partly reversed over Germany and France due to the modified cloud water path, solar radiation, and subsequently altered PBL height. Otherwise, the differences to the baseline case are quite similar to those found for case SI1. For spring and autumn, the situation was similar to that in summer.

In the winter, the extended area with increased NO₂ for AT1 does not appear to be related to differences in the mean PBL height between AT1 and the baseline. However, closer inspection of the diurnal course of the PBL heights shows that during winter the aerosol indirect effect results in lower PBL heights for AT1 than for the baseline in particular at night and in the morning. These conditions are more favorable for the nighttime accumulation of primary pollutants. The comparatively small increase in solar radiation during the daytime has almost no effect on the PBL height and NO₂ concentrations during this time. Accordingly, the increase in the mean NO₂ concentration in winter is mainly due to higher concentrations during the night (winter mean 0.6 ppb) and in the morning hours.

Ozone concentrations were found to be marginally lower for case SI1 than for the baseline over major parts of Europe during the summer. This can be partly attributed to lower photochemical activity and the reduction in solar radiation by the direct aerosol effect and to lower temperatures which lead to 2–3 % lower isoprene concentrations. The higher NO_x due to lower PBL heights also adds to this effect. However, except for Russia, this reduction is less than 0.2 ppb (Fig. 7). The most pronounced decrease was found for the region North-East of the Russian forest fire area. There, the summertime mean ozone was 1 ppb lower for SI1 than for the baseline case. Over the major parts of Northern Africa, the 0.4 ppb decrease in mean ozone can be almost completely related to lower photolysis and reaction rates due to the lack of isoprene and NO_x.

For investigation of the impact of the indirect aerosol effect on simulated near surface ozone, only case AT1 can be compared directly to SI1 and SI2. Over the North Atlantic, the summertime mean ozone was almost 2 ppb lower for AT1 than for the baseline case. In this area, the indirect aerosol effect resulted in strongly enhanced global radiation (Fig. 1) and photolysis frequencies (not shown). For low pollution levels, enhanced photochemical activity is known to result in ozone depletion (Murazaki and Hess, 2006).

For regions with high aerosol concentrations and low cloudiness, like Northern Africa and also Russia during the forest fire episode the patterns of ozone decrease reflect the patterns of the decrease in shortwave radiation due to the direct aerosol effect. There, the ozone decrease for case AT1 in the summer is similar to the ozone decrease for case SI1. For regions with lower aerosol concentrations, like Central Europe and parts of Scandinavia, the decrease in global radiation was less pronounced and the temperature was higher during summer for the cases AT1 and DE4 than for SI1 (Fig. 3 and Fig. S3). This changed the deviation of the isoprene concentration, which was negative for case SI1 to positive

for AT1 and DE4, which could be a reason for the increase in ozone for AT1.

In the winter, ozone concentrations that were up to 2 ppb lower were found over Central and Eastern Europe when the indirect aerosol effect was included. This may be related to the increased NO₂ over Central Europe (Fig. 6, 'AT1-SI2').

The pronounced differences between case DE4 and the baseline simulation are mostly not due to aerosol meteorology interactions, but due to modification of the gas phase chemistry solver. This modification has been introduced since the QSSA RADM2 solver supplied with WRF-Chem under-estimates ozone titration in the presence of high NO emissions. For example, simulations with CBM-Z (Supplement, Fig. S1) are able to reproduce this feature. Inspection of the NO₂ and ozone differences between DE4 and SI2 shown in Figs. 6 and 7 indicates that the modified solver yields a more pronounced ozone titration and lower NO₂ for the regions with high NO sources. However, elsewhere and in particular in the free troposphere (not shown) too high NO₂ concentrations developed during the year-long simulation. Nevertheless, Fig. 6 shows that, similar to AT1, the accumulation of NO₂ in the area from Northern Germany to the Baltic States in the winter as well as the associated depression of the ozone concentration also occurs in this case.

In spite of the changes in NO₂ and ozone patterns that may be related to specific aerosol feedbacks on atmospheric conditions, it must be concluded that on the average, the impact of the aerosol direct and indirect effect on ozone concentrations is below 5%, except for extreme events like the Russian 2010 wildfires.

3.2.2. PM₁₀ and PM_{2.5}

Aerosol concentrations were generally underestimated by up to 50%. This was the case not only for WRF-Chem but also for the majority of the models participating in the AQMEII phase2 model intercomparison. As reported by Balzarini et al. (2015) this can probably be attributed to the strong underestimation of organic compounds. MADE/SORGAM is known to under-predict secondary organic aerosol compounds (Ahmadov et al., 2012). Also, aerosol in the coarse mode is known to be under-predicted. On the other hand, near surface concentrations of aerosol sulfate, nitrate, and ammonium were overestimated for the case SI2.

Over Europe consideration of the direct aerosol effect results in an increase of PM₁₀ and PM_{2.5} by less than 5% (Figs. 8 and 9). Similar to the NO₂ concentrations, the deviations of the simulated PM concentrations between SI1 and the baseline case show a patchy pattern over the Russian wildfire area due to local disturbances of the wind speed and the PBL height reductions resulting from the strongly decreased solar radiation in this area. As also indicated by Fig. 8, inclusion of the direct aerosol effect essentially had no effect on the emissions and concentrations of sea salt over the North Atlantic and the Mediterranean. Changes in the sea salt concentrations were below 1 $\mu\text{g m}^{-3}$, which is also in line with the less than 1% deviations in wind speed (not shown) found there. Over North Africa, PM₁₀, which almost completely consists of mineral dust emissions in this area, is reduced by up to 2–5 $\mu\text{g m}^{-3}$. This can be attributed to 1–3% lower wind speeds there.

Inclusion of aerosol cloud interactions results in a further reduction of the already too low simulated PM₁₀ and PM_{2.5} by up to 50% compared to the baseline case. This decrease is related to removal by grid scale precipitation. Over the North Atlantic, the consideration of aerosol cloud interactions results in 20–50% lower PM₁₀ concentrations were found for cases AT1 and DE4, not only for the summer but throughout the year. Generally, patterns of differences to the baseline case were similar for AT1 and DE4. An

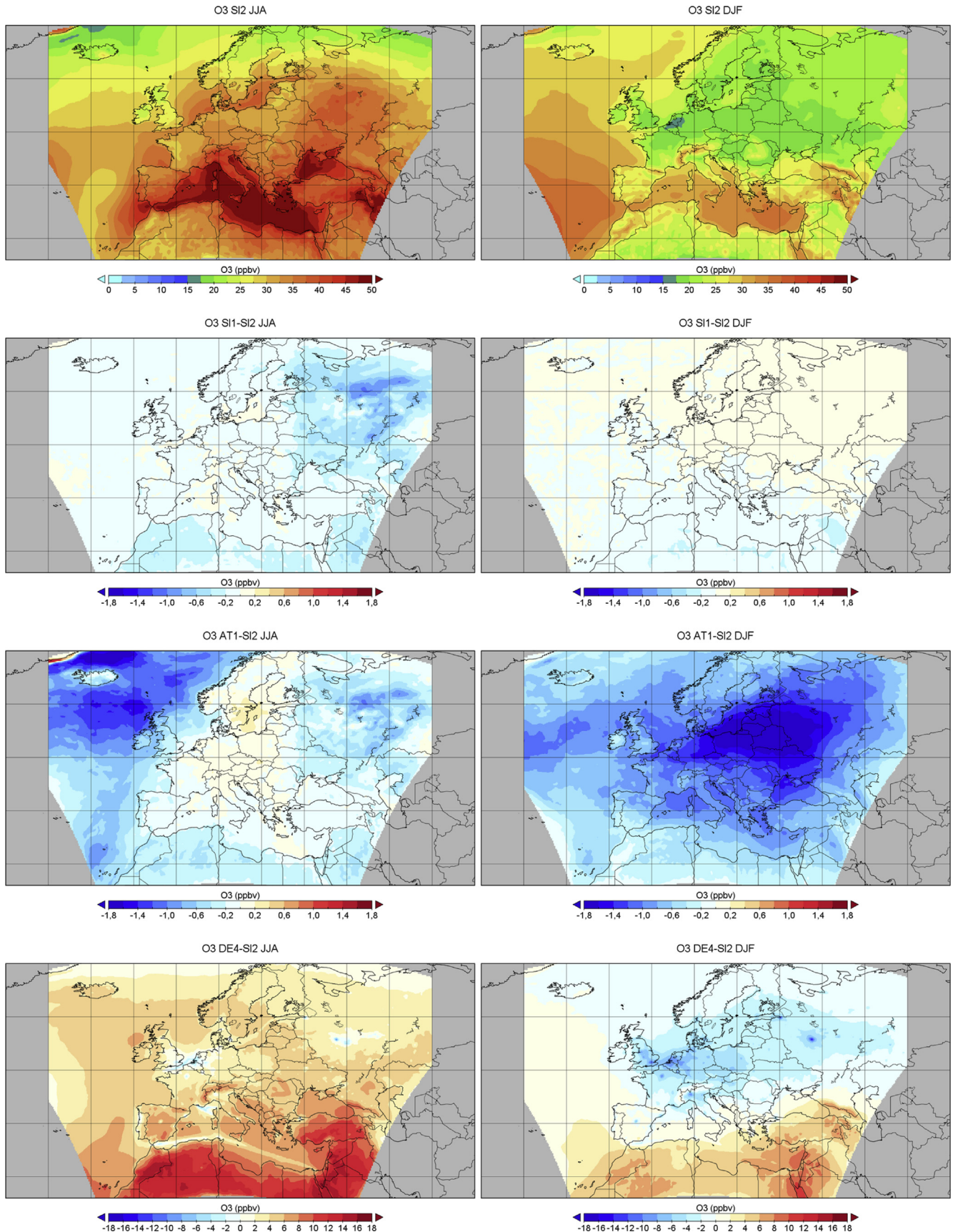


Fig. 7. Seasonal mean ozone concentration in ppbv for summer (left) and winter (right). From top to bottom: Baseline concentrations; difference between SI1 (direct aerosol effect) and baseline; difference between AT1 and baseline; difference between DE4 (same as AT1 but with different aqueous phase chemistry and modified gas phase solver) and baseline. Figures for DE4-SI2 are at different scale.

exception is the area over the Mediterranean, where stronger positive deviations were found for DE4 during summer.

Lower aerosol concentrations than for the baseline case were found for almost the entire modeling domain when the aerosol cloud interactions were included. In this way, the inclusion of aerosol cloud interactions worsens the already existing under-prediction of PM_{10} and $PM_{2.5}$ concentrations. On the other hand, too high aerosol sulfate, nitrate, and ammonium concentrations are simulated for cases SI1 and SI2. However, the enhanced removal of particulate matter for AT1 and DE4 results in too low aerosol sulfate (Im et al., 2015b). Further investigation is necessary to determine whether the removal of aerosol compounds is really overestimated in WRF-Chem when aerosol cloud interactions are explicitly considered or whether the higher negative bias is just a

consequence of the strongly underestimated organic and coarse aerosol concentrations.

4. Summary and conclusions

As a contribution to the AQMEII phase2 model intercomparison exercise eight different simulations for 2010 were performed with WRF-Chem for the European domain. In order to study the impact of the direct and indirect aerosol effect on predicted meteorological variables and on pollutant distributions, the simulations included different degrees of feedback, ranging from no aerosol effects at all to inclusion of the aerosol direct radiative effect together with aerosol cloud interactions and the aerosol indirect effect. The yearly simulations allow characterization of the average impact of the

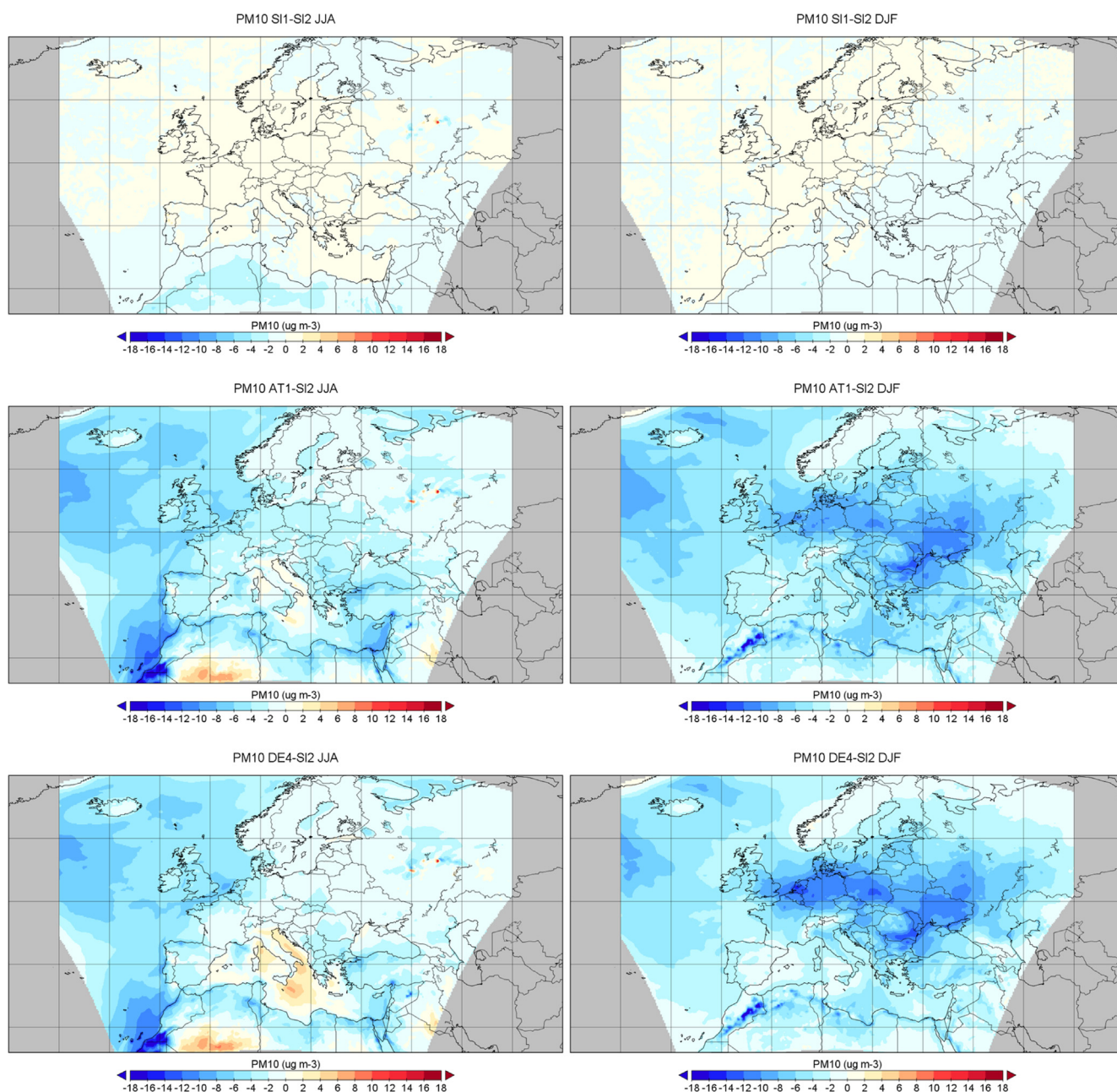


Fig. 8. Seasonal mean PM_{10} in $\mu\text{g m}^{-3}$ for summer (left) and winter (right). From top to bottom: Difference between SI1 and baseline; difference between AT1 and baseline; difference between DE4 (same as AT1 but with different aqueous phase chemistry and modified gas phase solver) and baseline. See Fig. 1 for the baseline concentrations.

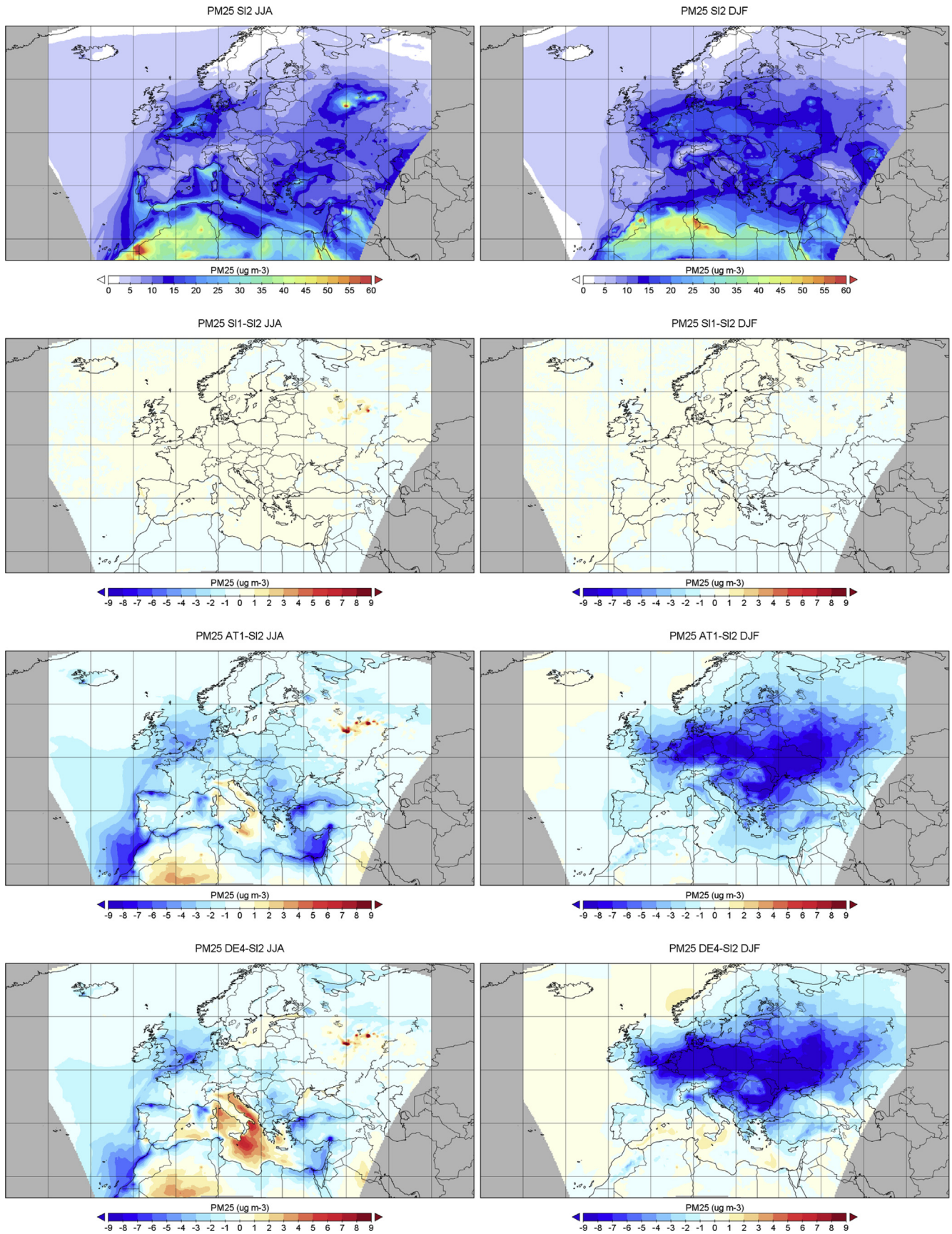


Fig. 9. Seasonal mean $\text{PM}_{2.5}$ concentration in $\mu\text{g m}^{-3}$ for summer (left) and winter (right). From top to bottom: Baseline concentrations; difference between SI1 and baseline; difference between AT1 and baseline; difference between DE4 (same as AT1 but with different aqueous phase chemistry) and baseline.

inclusion of feedback effects on the results air quality simulations and the analysis of seasonal behavior. The focus of the current analysis was on four simulations with RADM2 gas phase chemistry and the MADE/SORGAM aerosol module.

An intention of the current study was to investigate the impact of the aerosol direct and indirect effect on meteorology and pollutant concentrations without disturbance due to semi-direct effects, i.e. changes of the cloud distribution due to changes in the radiation budget. The common simulation strategy for AQMEII phase2, where the entire year 2010 was simulated as a sequence of two-day time slices, was found to successfully suppress the development of semi-direct effects under most conditions. An exception is the region of the Russian forest fires in July and August, where the strong attenuation of solar radiation due to high and temporally variable aerosol concentrations induced a faster development of semi-direct effects on single days.

Strong feedback effects were found for episodes and regions with extreme aerosol concentrations, like the 2010 Russian wildfires. Here, the direct aerosol effect lowered the seasonal mean solar radiation by 20 W m^{-3} and seasonal mean temperature by 0.25° . This might be considered a lower limit as it must be taken into account that aerosol concentrations were generally underestimated by up to 50%.

The most pronounced feedback effects due to the indirect effect were found for regions with very low aerosol concentrations like the Atlantic and Northern Europe. There, the predicted low aerosol concentrations result in very low cloud droplet numbers and a reduced cloud liquid water path. The consequence is an increase of the downward solar radiation by almost 50%, leading to almost one degree higher mean temperatures in the summer over Northern Scandinavia. In the winter, the decreased liquid water path leads to enhanced long-wave cooling with a decrease of the simulated mean temperature over Scandinavia. In summary, the direct aerosol effect leads to lower temperatures and PBL heights for all seasons whereas the impact of the aerosol indirect effect on temperature over Northern Europe depends strongly on the season.

Up to 30% higher simulated precipitation over the Atlantic Ocean was simulated when cloud droplet formation accounts for predicted aerosol concentrations. Previous tests indicated that this effect will still persist for aerosol concentrations that are twice as high as those simulated here. The decrease of cloud water path and the increased global radiation over the Atlantic and Northern Europe when the indirect aerosol effect is included was found to be the most robust feature of the WRF-Chem simulations and was persistent for all seasons. Due to the high aerosol concentrations from the emissions of the 2010 wildfires, 10%–30% lower precipitation was simulated for Russia during the summer when aerosol cloud interactions were taken into account. The inclusion of aerosol cloud interactions was found to reduce the bias or improve correlations of simulated precipitation for some episodes and regions, for example for the North Atlantic and Russia during summer. However, the domain- and time-averaged performance statistics do not indicate a general improvement when aerosol feedbacks are taken into account.

With some exceptions, the impact of aerosol feedbacks on simulated pollutant distributions was smaller than the effect of the choice of the chemistry mechanism and the aerosol module. For the gas phase chemistry, this was also confirmed by [Knote et al. \(2015a\)](#). Like for the majority of the models participating in the AQMEII phase2 model intercomparison, a strong underestimation of the aerosol concentrations was also found for the WRF-Chem simulations. The inclusion of aerosol cloud interactions even worsened the under-prediction of PM_{10} and PM_2 as it resulted in 50% lower aerosol concentrations than for the baseline case. Further investigation is required to determine whether the removal of aerosol compounds is

really overestimated by WRF-Chem when aerosol cloud interactions are explicitly considered or whether the higher negative bias is just a consequence of the strongly underestimated organic and coarse aerosol concentrations for the baseline case.

No general statement on the performance of WRF-Chem will be given here, as simulation results depend strongly on the configuration and the chosen physics and chemistry options. One exception is WRF-Chem's RADM2 QSSA solver and the modification of this solver that was tested here. Although the modification of the solver sometimes resulted in a smaller ozone bias for DE4 than for the simulations with the unchanged RADM2 solver ([Im et al., 2015a](#)), an outcome of the AQMEII phase2 model intercomparison was that this modification cannot be recommended, as it overestimates NO_2 and ozone for low NO_x conditions. Due to the high bias of simulated ozone concentration for regions with strong NO sources that is found when WRF-Chem's original RADM2 solver is applied, this solver cannot be recommended either. WRF-Chem users who want to continue using the RADM2 mechanism are recommended to change to one of WRF-Chem's KPP options for RADM2.

The results related to aerosol feedbacks on meteorology and pollutant distributions depend generally on the model configuration, i.e. on the baseline aerosol and the cloud droplet numbers that are assumed in the model if no predicted aerosol concentrations are used for the calculation of cloud droplet formation. In the WRF-Chem version 3.4.1 used here, continental conditions are implicitly assumed for the entire modeling domain when cloud droplet numbers are not explicitly calculated from predicted aerosol particle numbers. The current simulations indicate that this assumption as a strong effect on cloud water content and subsequent global radiation fields as it results for clean conditions in much higher cloud water contents and less precipitation as compared to simulations where simulated aerosol concentrations are considered for aerosol cloud interactions. The use of climatological aerosol fields instead of horizontally homogeneous particle numbers can certainly improve simulated cloud water concentrations and global radiation fields for clean conditions if no simulated aerosol concentrations are available. Differences between simulations with aerosol cloud interactions depending on simulated aerosol concentrations and the baseline would certainly be less pronounced if climatological aerosol fields are applied for the baseline case. On the other hand, effects may become more pronounced if aerosol cloud interactions are also included in the sub-grid convective cloud parameterizations.

Acknowledgments

We gratefully acknowledge the contribution of various groups to the second air Quality Model Evaluation international Initiative (AQMEII) activity: TNO (anthropogenic emissions database); ECMWF/MACC project & Météo-France/CNRM-GAME (chemical boundary conditions), and the Finnish Meteorological Institute FMI (fire emissions). Joint Research Center Ispra/Institute for Environment and Sustainability provided its ENSEMBLE system for model output harmonization and analyses, and evaluation. The UPM authors thankfully acknowledge the computer resources, technical expertise and assistance provided by the Centro de Supercomputación y Visualización de Madrid (CESVIMA) and the Spanish Supercomputing Network (BSC). The UMU group acknowledges the funding from the project CGL2013-48491-R, Spanish Ministry of Economy and Competitiveness. The Centre of Excellence for Space Sciences and Technologies SPACE-SI is an operation partly financed by the European Union, European Regional Development Fund grant OP13.1.1.2.02.0004 and Republic of Slovenia, Ministry of Higher Education, Science, Sport and Culture. The co-ordination

and support of the European contribution through COST Action ES1004 EuMetChem and the support of IMK-IFU by REKLIM is gratefully acknowledged.

Appendix. Modification of the RADM2 solver in WRF-Chem

Within the QSSA chemistry solver for RADM2 that is implemented in WRF-Chem the concentration of NO, C_{NO} , is calculated diagnostically from the concentration of NO_x , C_{NO_x} , and the concentration of NO_2 , C_{NO_2} :

$$C_{NO} = C_{NO_x} / (\text{Prod}_{NO} / \text{Loss}_{NO} + C_{NO_2}) \quad (\text{A1})$$

The concentrations C_{NO_x} and C_{NO_2} have been calculated from the prognostic differential equations before. The NO_2 concentration is then re-calculated by the following relationship:

$$C_{NO_2} = C_{NO_2} * C_{NO_x} / (\text{Prod}_{NO} / \text{Loss}_{NO} + C_{NO_2}) \quad (\text{A2})$$

Prod_{NO} and Loss_{NO} are the production and loss reactions for NO as given by Stockwell et al. (1990).

This treatment was found to result in an under-representation of nocturnal ozone titration for areas with high NO emissions.

Therefore, the above treatment was replaced for the DE4 simulation simply by:

$$C_{NO} = C_{NO_x} - C_{NO_2} \quad (\text{A3})$$

Although (A3) seemed to perform well when short episodes are simulated and for polluted areas, it turned out during the AQMEII phase2 application that this simple approach tends to overestimate the NO_2 concentration for pristine regions and in the free troposphere, which resulted in an overestimation of ozone. This became particularly evident as the AQMEII domain includes large areas with very low NO_2 , such as parts of the Atlantic and the Sahara desert.

Due to the deficiencies of both approaches, we recommend choosing options with the KPP solver instead of the QSSA solver for WRF-Chem simulations with the RADM2 mechanism.

Appendix A. Supplementary data

Supplementary data related to this article can be found at <http://dx.doi.org/10.1016/j.atmosenv.2014.10.056>.

References

- Abdul-Razzak, H., Ghan, S.J., 2002. A parameterization of aerosol activation 3: sectional representation. *J. Geophys. Res.* 107 (D3) <http://dx.doi.org/10.1029/2001JD000483>. AAC-1-1–AAC1-6.
- Ackermann, I.J., Hass, H., Memmesheimer, M., Ebel, A., Binkowski, F.S., Shankar, U., 1998. Modal aerosol dynamics model for Europe: development and first applications. *Atmos. Environ.* 32, 2981–2999.
- Ahmadov, R., McKeen, S.A., Robinson, A.L., Bahreini, R., Middlebrook, A.M., de Gouw, J.A., Meagher, J., Hsie, E.-Y., Edgerton, E., Shaw, S., Trainer, M., 2012. A volatility basis set model for summertime secondary organic aerosols over the eastern United States in 2006. *J. Geophys. Res.* 117, D06301.
- Alapaty, K., Mathur, R., Pleim, J., Hogrefe, C., Rao, S.T., 2012. New directions: understanding interactions of air quality and climate change at regional scales. *Atmos. Environ.* 49, 419–421.
- Andreae, M.O., Merlet, P., 2001. Emission of trace gases and aerosols from biomass burning. *Glob. Biogeochem. Cycles* 15, 955–966.
- Baklanov, A., Schlünzen, K., Suppan, P., Baldasano, J., Brunner, D., Aksoyoglu, S., Carmichael, G., Douros, J., Flemming, J., Forkel, R., Galmarini, S., Gauss, M., Grell, G., Hirtl, M., Joffre, S., Jorba, O., Kaas, E., Kaasik, M., Kallos, G., Kong, X., Korsholm, U., Kurganskiy, A., Kushta, J., Lohmann, U., Mahura, A., Manders-Groot, A., Maurizi, A., Moussiopoulos, N., Rao, S.T., Savage, N., Seigneur, C., Sokhi, R.S., Solazzo, E., Solomos, S., Sørensen, B., Tsegas, G., Vignati, E., Vogel, B., Zhang, Y., 2014. Online coupled regional meteorology chemistry models in

- Europe: current status and prospects. *Atmos. Chem. Phys.* 14, 317–398. <http://dx.doi.org/10.5194/acp-14-317-2014>.
- Balzarini, A., Pirovano, G., Honzak, L., Žabkar, R., Curci, G., Forkel, R., Hirtl, M., San José, R., Tuccella, P., Grell, G., 2015. WRF-Chem model sensitivity to chemical mechanisms choice in reconstructing aerosol optical properties. *Atmos. Environ.* 115, 604–619.
- Bangert, M., Kottmeier, C., Vogel, B., Vogel, H., 2011. Regional scale effects of the aerosol cloud interaction simulated with an online coupled comprehensive chemistry model. *Atmos. Chem. Phys.* 11 <http://dx.doi.org/10.5194/acp-11-4411-2011>.
- Bangert, M., Nenes, A., Vogel, B., Vogel, H., Barahona, D., Karydis, V.A., Kumar, P., Kottmeier, C., Blahak, U., 2012. Saharan dust event impacts on cloud formation and radiation over Western Europe. *Atmos. Chem. Phys.* 12, 4045–4063. <http://dx.doi.org/10.5194/acp-12-4045-2012>.
- Baró, R., Jiménez-Guerrero, P., Balzarini, A., Curci, G., Forkel, R., Hirtl, M., Honzak, L., Im, U., Lorenz, C., Pérez, J.L., Pirovano, G., San José, R., Tuccella, P., Werhahn, J., Žabkar, R., 2015. Sensitivity analysis of the microphysics scheme in WRF-Chem contributions to AQMEII phase2. *Atmos. Environ.* 115, 620–629.
- Bianconi, R., Galmarini, S., Bellasio, R., 2004. Web-based system for decision support in case of emergency: ensemble modelling of long-range atmospheric dispersion of radionuclides. *Environ. Model. Softw.* 19, 401–411.
- Brunner, D., Eder, B., Jorba, O., Savage, N., Makar, P., Giordano, L., Badia, A., Balzarini, A., Baro, R., Chemel, C., Forkel, R., Jimenez-Guerrero, P., Hirtl, M., Hodzic, A., Honzak, L., Knote, C., Kuenen, J.J.P., Makar, P.A., Manders-Groot, A., Davis, L., Perez, J.L., Pirovano, G., San Jose, R., Savage, N., Schroder, W., Sokhi, R.S., Syrakov, D., Torian, A., Werhahn, K., Wolke, R., Yahya, K., Zabkar, R., Zhang, Y., Zhang, J., Hogrefe, C., Galmarini, S., 2015. Comparative analysis of meteorological performance of coupled chemistry-meteorology models in the context of AQMEII phase 2. *Atmos. Environ.* 115, 470–498.
- Chapman, E.G., Gustafson Jr., W.L., Easter, R.C., Barnard, J.C., Ghan, S.J., Pekour, M.S., Fast, J.D., 2009. Coupling aerosol-cloud-radiative processes in the WRF-Chem model: investigating the radiative impact of elevated point sources. *Atmos. Chem. Phys.* 9, 945–964.
- Charlson, R.J., Schwartz, S.E., Hales, J.M., Cess, R.D., Coakley Jr., J.A., Hansen, J.E., Hofmann, D.J., 1992. Climate forcing by anthropogenic aerosols. *Science* 255 (5043), 423–430. <http://dx.doi.org/10.1126/science.255.5043.423>.
- Chen, F., Dudhia, J., 2001. Coupling an advanced land surface-hydrology model with the Penn State-NCAR MM5 modeling system. Part I: model implementation and sensitivity. *Mon. Weather Rev.* 129, 569–585.
- Easter, R.C., Ghan, S., Zhang, J.Y., Saylor, R.D., Chapman, E.G., Laulainen, N.S., Abdul-Razzak, H., Leung, L.R., Bian, X., Zaveri, R.A., 2004. MIRAGE: model description and evaluation of aerosols and trace gases. *J. Geophys. Res.* 109 <http://dx.doi.org/10.1029/2004JD004571>.
- Fahey, K.M., Pandis, S.N., 2001. Optimizing model performance: variable size resolution in cloud chemistry modeling. *Atmos. Environ.* 35, 4471–4478.
- Fast, J.D., Gustafson Jr., W.L., Easter, R.C., Zaveri, R.A., Barnard, J.C., Chapman, E.G., Grell, G.A., Peckham, S.E., 2006. Evolution of ozone, particulates, and aerosol direct radiative forcing in the vicinity of Houston using a fully coupled meteorology-chemistry-aerosol model. *J. Geophys. Res.* 111, D21305. <http://dx.doi.org/10.1029/2005JD006721>.
- Forkel, R., Werhahn, J., Buus Hansen, A., McKeen, S., Peckham, S., Grell, G., Suppan, P., 2012. Effect of aerosol-radiation feedback on regional air quality – a case study with WRF/Chem. *Atmos. Environ.* 53, 202–211. <http://dx.doi.org/10.1016/j.atmosenv.2011.10.009>.
- Galmarini, S., Bianconi, R., Appel, W., Solazzo, E., Mosca, S., Grossi, P., Moran, M., Schere, K., Rao, S.T., 2012. ENSEMBLE and AMET: two systems and approaches to a harmonized, simplified and efficient facility for air quality models development and evaluation. *Atmos. Environ.* 53, 51–59.
- Grell, G.A., Baklanov, A., 2011. Integrated modeling for forecasting weather and air quality: a call for fully coupled approaches. *Atmos. Environ.* 45, 6845–6851. <http://dx.doi.org/10.1016/j.atmosenv.2011.01.017>.
- Grell, G.A., Devenyi, D., 2002. A generalized approach to parameterizing convection combining ensemble and data assimilation techniques. *Geophys. Res. Lett.* 29 (14) <http://dx.doi.org/10.1029/2002GL015311>.
- Grell, G., Emeis, S., Stockwell, W.R., Schoenemeyer, T., Forkel, R., Michalakes, J., Knoche, R., Seidl, W., 2000. Application of a multiscale, coupled MM5/chemistry model to the complex terrain of the VOTALP valley campaign. *Atmos. Environ.* 34, 1435–1453.
- Grell, G.A., Knoche, R., Peckham, S.E., McKeen, S.A., 2004. Online versus offline air quality modeling on cloud-resolving scales. *Geophys. Res. Lett.* 31, L16117. <http://dx.doi.org/10.1029/2004GL020175>.
- Grell, G.A., Peckham, S.E., Schmitz, R., McKeen, S.A., Frost, G., Skamarock, W.C., Eder, B., 2005. Fully coupled online chemistry within the WRF model. *Atmos. Environ.* 39, 6957–6975.
- Grell, G., Freitas, S.R., Stuefer, M., Fast, J., 2011. Inclusion of biomass burning in WRF-Chem: impact of wildfires on weather forecasts. *Atmos. Chem. Phys.* 11, 5289–5303. <http://dx.doi.org/10.5194/acp-11-5289-2011>.
- Guenther, A., Karl, T., Harley, P., Wiedinmyer, C., Palmer, P.I., Geron, C., 2006. Estimates of global terrestrial isoprene emissions using MEGAN (Model of Emissions of Gases and Aerosols from Nature). *Atmos. Chem. Phys.* 6, 3181–3210.
- Haylock, M.R., Hofstra, N., Klein Tank, A.M.G., Klok, E.J., Jones, P.D., New, M., 2008. A European daily gridded dataset of surface temperature and precipitation. *J. Geophys. Res.* 113, D20119. <http://dx.doi.org/10.1029/2008JD10201>.

- Hong, S., Noh, Y., Dudhia, J., 2006. A new vertical diffusion package with an explicit treatment of entrainment processes. *Mon. Weather Rev.* 134, 2318–2341.
- Iacono, M.J., Delamere, J.S., Mlawer, E.J., Shephard, M.W., Clough, S.A., Collins, W.D., 2008. Radiative forcing by long-lived greenhouse gases: calculations with the AER radiative transfer models. *J. Geophys. Res.* 113, D13103.
- Im, U., Bianconi, R., Solazzo, E., Kioutsioukis, I., Badia, A., Balzarini, A., Baró, R., Bellasio, R., Brunner, D., Chemel, C., Curci, G., Flemming, J., Forkel, R., Giordano, L., Jimenez-Guerrero, P., Hirtl, M., Hodzic, A., Honzak, L., Jorba, O., Knote, C., Kuenen, J.J.P., Makar, P.A., Manders-Groot, A., Neal, L., Perez, J.L., Pirovano, G., Pouliot, G., San Jose, R., Savage, N., Schroder, W., Sokhi, R.S., Syrakov, D., Torian, A., Tuccella, P., Werhahn, K., Wolke, R., Yahya, K., Zabkar, R., Zhang, Y., Zhang, J., Hogrefe, C., Galmarini, S., 2015a. Evaluation of operational online-coupled regional air quality models over Europe and North America in the context of AQMEII phase2. Part I: ozone. *Atmos. Environ.* 115, 404–420.
- Im, U., Bianconi, R., Solazzo, E., Kioutsioukis, I., Badia, A., Balzarini, A., Baró, R., Bellasio, R., Brunner, D., Chemel, C., Curci, G., Denier van der Gon, H., Flemming, J., Forkel, R., Giordano, L., Jiménez-Guerrero, P., Hirtl, M., Hodzic, A., Honzak, L., Jorba, O., Knote, C., Makar, P.A., Manders-Groot, A., Neal, L., Pérez, J.L., Pirovano, G., Pouliot, G., San Jose, R., Savage, N., Schroder, W., Sokhi, R.S., Syrakov, D., Torian, A., Tuccella, P., Wang, K., Werhahn, J., Wolke, R., Zabkar, R., Zhang, Y., Zhang, J., Hogrefe, C., Galmarini, S., 2015b. Evaluation of operational online-coupled regional air quality models over Europe and North America in the context of AQMEII phase2. Part II: particulate matter. *Atmos. Environ.* 115, 421–441.
- Inness, A., Baier, F., Benedetti, A., Bouarar, I., Chabrilat, S., Clark, H., Clerbaux, C., Coheur, P., Engelen, R.J., Errera, Q., Flemming, J., George, M., Granier, C., Hadji-Lazarou, J., Huijnen, V., Hurtmans, D., Jones, L., Kaiser, J.W., Kapsomenakis, J., Lefever, K., Leitão, J., Razinger, M., Richter, A., Schultz, M.G., Simmons, A.J., Suttie, M., Stein, O., Thépaut, J.-N., Thouret, V., Vrekoussis, M., Zerefos, C., the MACC Team, 2013. The MACC reanalysis: an 8 yr data set of atmospheric composition. *Atmos. Chem. Phys.* 13, 4073–4109.
- Jacobson, M.Z., 1997. Development and application of a new air pollution modeling system, part III: aerosol-phase simulations. *Atmos. Environ.* 31, 587–608.
- Jimenez, P., Dudhia, J., 2012. Improving the representation of resolved and unresolved topographic effects on surface wind in the WRF Model. *J. Appl. Meteorol. Climatol.* 51, 300–316. <http://dx.doi.org/10.1175/JAMC-D-11-084.1>
- Knote, C., Tuccella, P., Curci, G., Emmons, L., Orlando, J.J., Madronich, S., Baró, R., Jiménez-Guerrero, P., Lueken, D., Hogrefe, C., Forkel, R., Werhahn, J., Hirtl, M., Pérez, J.L., San José, R., Giordano, L., Brunner, D., Khairunnisa, Y., Zhang, Y., 2015. Influence of the choice of gas-phase mechanism on predictions of key gaseous pollutants during the AQMEII phase-2 intercomparison. *Atmos. Environ.* 115, 553–568.
- Kong, X., Forkel, R., Sokhi, R.S., Suppan, P., Baklanov, A., Gauss, M., Brunner, D., Baró, R., Balzarini, A., Chemel, C., Curci, G., Guerrero, P.J., Hirtl, M., Honzak, L., Im, U., Pérez, J.L., Pirovano, G., San Jose, R., Schlünzen, K.H., Tsegas, G., Tuccella, P., Werhahn, J., Zabkar, R., Galmarini, S., 2015. Analysis of meteorology-chemistry interactions during air pollution episodes using online coupled models within AQMEII phase2. *Atmos. Environ.* 115, 527–540.
- Korsholm, U.S., Baklanov, A., Gross, A., Mahura, A., Sass, B.H., Kaas, E., 2008. Online coupled chemical weather forecasting based on HIRLAM – overview and perspective of Enviro-HIRLAM. *HIRLAM Newsl.* 54, 151–168. Available at: http://hirlam.org/index.php?option=com_docman&task=docdownload&gid=148&Itemid=70 (last accessed 11.02.11).
- Kuenen, J.J.P., Visschedijk, A.J.H., Jozwicka, M., Denier van der Gon, H.A.C., 2014. TNO_MACC_II emission inventory: a multi-year (2003–2009) consistent high-resolution European emission inventory for air quality modelling. *Atmos. Chem. Phys.* 14, 10963–10976. <http://dx.doi.org/10.5194/acp-14-10963-2014>.
- Kushta, J., Kallos, G., Astitha, M., Solomos, S., Spyrou, C., Mitsakou, C., Lelieveld, J., 2014. Impact of natural aerosols on atmospheric radiation and consequent feedbacks with the meteorological and photochemical state of the atmosphere. *J. Geophys. Res.* 119, 1463–1491. <http://dx.doi.org/10.1002/2013JD020714>.
- Lin, Y.-L., Farley, R.D., Orville, H.D., 1983. Bulk parameterization of the snow field in a cloud model. *J. Appl. Meteorol.* 22, 1065–1092.
- Makar, P.A., Gong, W., Milbrandt, J., Hogrefe, C., Zhang, Y., Curci, G., Zakbar, R., Im, U., Galmarini, S., Gravel, S., Zhang, J., Hou, A., Pabla, B., Cheung, P., Bianconi, R., 2015a. Feedbacks between air pollution and weather, part 1: effects on weather. *Atmos. Environ.* 115, 442–469.
- Makar, P.A., Gong, W., Hogrefe, C., Zhang, Y., Curci, G., Zabkar, R., Milbrandt, J., Im, U., Galmarini, S., Balzarini, A., Baró, R., Bianconi, R., Cheung, P., Forkel, R., Gravel, S., Hirtl, M., Honzak, L., Hou, A., Jimenez-Guerrero, P., Langer, M., Moran, M.D., Pabla, B., Perez, P.L., Pirovano, G., San Jose, R., Tuccella, P., Werhahn, J., Zhang, J., 2015b. Feedbacks between air pollution and weather, part 2: effects on chemistry. *Atmos. Environ.* 115, 499–526.
- Mass, C., Owens, D., 2011. Fixing WRF's high speed wind bias: a new subgrid scale drag parameterization and the role of detailed verification. In: Abstracts of the 91st AMS Annual Meeting, Seattle, WA, 23–27 Jan 2011, p. 2011, 2019B. 2016. Available at: <http://ams.confex.com/ams/91Annual/webprogram/Paper180011.html>.
- Mathur, R., Pleim, J., Wong, D., Otte, T., Gilliam, R., Roselle, S., Young, J., Binkowski, F., Xiu, A., 2010. The WRF-CMAQ integrated on-line modeling system: development, testing, and initial applications. In: *Air Pollution Modeling and its Application XX*. Springer, pp. 155–159.
- Morrison, H., Thompson, G., Tatarskii, V., 2009. Impact of cloud microphysics on the development of trailing stratiform precipitation in a simulated squall line: comparison of one- and two-moment schemes. *Mon. Weather Rev.* 137, 991–1007. <http://dx.doi.org/10.1175/2008MWR2556.1>.
- Murazaki, K., Hess, P., 2006. How does climate change contribute to surface ozone change over the United States? *J. Geophys. Res.* 111. <http://dx.doi.org/10.1029/2005JD005873>. D05301.
- Pouliot, G., Pierce, T., Denier van der Gon, H., Schaap, M., Moran, M., Nopmongkol, U., 2012. Comparing emissions inventories and model-ready emissions datasets between Europe and North America for the AQMEII project. *Atmos. Environ.* 53, 75–92.
- Pouliot, G., Denier van der Gon, H., Kuenen, J., Makar, P., Zhang, J., Moran, M., 2015. Analysis of the Emission Inventories and Model-Ready Emission Datasets of Europe and North America for Phase 2 of the AQMEII Project. *Atmos. Environ.* 115, 345–360.
- Rao, S.T., Galmarini, S., Puckett, K., 2011. Air quality model evaluation international initiative (AQMEII): advancing the state of the science in regional photochemical modeling and its applications. *BAMS* 92, 23–30.
- San José, R., Pérez, J.L., Balzarini, A., Baró, R., Curci, G., Forkel, R., Galmarini, S., Grell, G., Hirtl, M., Honzak, L., Im, U., Jiménez-Guerrero, P., Langer, M., Pirovano, G., Tuccella, P., Werhahn, J., Zabkar, R., 2015. Sensitivity of feedback effects in CBMZ/MOSAIC chemical mechanism. *Atmos. Environ.* 115, 646–656.
- Schell, B., Ackermann, I.J., Hass, H., Binkowski, F.S., Ebel, A., 2001. Modeling the formation of secondary organic aerosol within a comprehensive air quality model system. *J. Geophys. Res.* 106, 28275–28293.
- Shaw, W.J., Allwine, K., Fritz, B.G., Rutz, F.C., Rishel, J.P., Chapman, E.G., 2008. An evaluation of the wind erosion module in DUSTAN. *Atmos. Environ.* 42, 1907–1921.
- Sofiev, M., Vankevich, R., Lotjonen, M., Prank, M., Petukhov, V., Ermakova, T., Koskinen, J., Kukkonen, J., 2009. An operational system for the assimilation of the satellite information on wild-land fires for the needs of air quality modelling and forecasting. *Atmos. Chem. Phys.* 9, 6833–6847. <http://dx.doi.org/10.5194/acp-9-6833-2009>.
- Solazzo, E., Bianconi, R., Vautard, R., Wyatt Appel, K., Moran, M.D., Hogrefe, C., Bessagnet, B., Brandt, J., Christensen, J.H., Chemel, C., Coll, I., van der Gon, H.D., Ferreira, J., Forkel, R., Francis, X.V., Grell, G., Grossi, P., Hansen, A.B., Jericevic, A., Kraljevic, L., Miranda, A.I., Nopmongcol, U., Pirovano, G., Prank, M., Riccio, A., Sartelet, K.N., Schaap, M., Silver, J.D., Sokhi, R.S., Vira, J., Werhahn, J., Wolke, R., Yarwood, G., Zhang, J., Rao, S.T., Galmarini, S., 2012(a). Model evaluation and ensemble modelling of surface-level ozone in Europe and North America in the context of AQMEII. *Atmos. Environ.* 53, 60–74.
- Solazzo, E., Bianconi, R., Pirovano, G., Matthias, V., Vautard, R., Moran, M.D., Appel, K.W., Bessagnet, B., Brandt, J., Christensen, J.H., Chemel, C., Coll, I., Ferreira, J., Forkel, R., Francis, X.V., Grell, G., Grossi, P., Hansen, A.B., Miranda, A.I., Nopmongcol, U., Prank, M., Sartelet, K.N., Schaap, M., Silver, J.D., Sokhi, R.S., Vira, J., Werhahn, J., Wolke, R., Yarwood, G., Zhang, J., Rao, S.T., Galmarini, S., 2012b. Operational model evaluation for particulate matter in Europe and North America in the context of AQMEII. *Atmos. Environ.* 53, 75–92.
- Solomos, S., Kallos, G., Kushta, J., Astitha, M., Tremback, C., Nenes, A., Levin, Z., 2011. An integrated modeling study on the effects of mineral dust and sea salt particles on clouds and precipitation. *Atmos. Chem. Phys.* 11, 873–892. <http://dx.doi.org/10.5194/acp-11-873-2011>.
- Stockwell, W.R., Middleton, P., Chang, J.S., Tang, X., 1990. The second generation regional acid deposition model chemical mechanism for regional air quality modeling. *J. Geophys. Res.* 95, 16343–16367.
- Stockwell, W.R., Kirchner, F., Kuhn, M., Seefeld, S., 1997. A new mechanism for regional atmospheric chemistry modeling. *J. Geophys. Res.* 102, 25847–25879. <http://dx.doi.org/10.1029/97JD00849>.
- Twomey, S., 1974. Pollution and the planetary albedo. *Atmos. Environ.* 8, 1251–1256.
- Vogel, B., Vogel, H., Bäumer, D., Bangert, M., Lundgren, K., Rinke, R., Stanelle, T., 2009. The comprehensive model system COSMO-ART – radiative impact of aerosol on the state of the atmosphere on the regional scale. *Atmos. Chem. Phys.* 9, 8661–8680. <http://dx.doi.org/10.5194/acp-9-8661-2009>.
- Walcek, C.J., Taylor, G.R., 1986. A theoretical model for computing vertical distributions of acidity and sulfate production within cumulus clouds. *J. Atmos. Sci.* 43, 339–355.
- Wiedinmyer, C., Akagi, S.K., Yokelson, R.J., Emmons, L.K., Al-Saadi, J.A., Orlando, J.J., Soja, A.J., 2011. The Fire INventory from NCAR (FINN): a high resolution global model to estimate the emissions from open burning. *Geosci. Model Dev.* 4, 625–641. <http://dx.doi.org/10.5194/gmd-4-625-2011>.
- Wild, O., Zhu, X., Prather, M.J., 2000. Fast-J: accurate simulation of in- and below cloud photolysis in tropospheric chemical models. *J. Atmos. Chem.* 37, 245–282.
- Yang, Q., Gustafson Jr., W.I., Fast, J.D., Wang, H., Easter, R.C., Morrison, H., 2011. Assessing regional scale predictions of aerosols, marine stratocumulus, and their interactions during VOCALS-REX using WRF-Chem. *Atmos. Chem. Phys.* 11, 11951–11975. <http://dx.doi.org/10.5194/acp-11-22663-2011>.
- Zaveri, R.A., Peters, L.K., 1999. A new lumped structure photochemical mechanism for largescale applications. *J. Geophys. Res.* 104, 30387–30415.
- Zaveri, R.A., Easter, R.C., Fast, J.D., Peters, L.K., 2008. Model for simulating aerosol interactions and chemistry (MOSAIC). *J. Geophys. Res.* 113, D13204. <http://dx.doi.org/10.1029/2007JD008782>.
- Zhang, Y., 2008. Online-coupled meteorology and chemistry models: history, current status, and outlook. *Atmos. Chem. Phys.* 8, 2895–2932.